Universitat Autònoma de Barcelona

Design and characterization of dense and porous Fe-based alloys for biomedical and environmental applications

Yuping Feng

Universitat Autònoma
de Barcelona

Design and characterization of dense and porous Fe-based alloys for biomedical and environmental applications

Yuping Feng

Tesi Doctoral

Programa de Doctorat en Ciència de Materials

Jordi Sort Viñas (director i tutor)

Eva Pellicer Vilà (directora)

Jordina Fornell Beringues (directora)

Departament de Física

Facultat de Ciències

2017

Universitat Autònoma
de Barcelona

Memòria presentada per aspirar al Grau de Doctor per

Yuping Feng

Vist i plau

Prof. Jordi Sort Viñas
(director i tutor)

Dra. Eva Pellicer Vilà	Dra. Jordina Fornell Beringues
(directora)	(directora)

Bellaterra, 14/09/2017

UAB
Universitat Autònoma
de Barcelona

Gnm3
Group of smart nanoengineered materials, nanomechanics and nanomagnetism

El **Prof. Jordi Sort Viñas**, professor ICREA del Departament de Física de la Universitat Autònoma de Barcelona,

La **Dra. Eva Pellicer Vilà**, investigadora Ramón y Cajal del Departament de Física de la Universitat Autònoma de Barcelona,

i la **Dra. Jordina Fornell Beringues**, investigadora Juan de la Cierva del Departament de Física de la Universitat Autònoma de Barcelona,

CERTIFIQUEN:

Que **Yuping Feng** ha realitzat sota la seva direcció el treball d'investigació que s'exposa a la memòria titulada "*Design and characterization of dense and porous Fe-based alloys for biomedical and environmental applications*" per optar al grau de **Doctor per la Universitat Autònoma de Barcelona**.

Que el disseny dels experiments, síntesi de mostres, llur caracterització, l'anàlisi dels resultats, la redacció dels articles i d'aquesta memòria són fruit del treball d'investigació realitzat per Yuping Feng.

I perquè així consti, signen el present certificat,

Prof. Jordi Sort Viñas

Dra. Eva Pellicer Vilà

Dra. Jordina Fornell Beringues

Bellaterra, 14 de setembre de 2017

Acknowledgements

I would first like to thank my supervisors Dr. Eva Pellicer and Prof. Jordi Sort for their valuable guidance, support and advices, not only in the scientific area, but also on a personal level. I would also like to thank Dr. Jordina Fornell, who helped me a lot regarding experimental skills, academic writing and presentation skills. In a word, thanks to all of them for broadening my horizons on biomaterials science and magnetism fields.

I would like to give a special appreciation to Dr. Huiyan Zhang and Dr. Jin Zhang. Thanks to Jin for her help on everything when I face problems abroad. Thanks to Huiyan for her encouragement and explanation when I became confused with research work.

I am grateful to all co-authors of the articles I have published or submitted so far.

I would also like to thank all the colleagues for their wonderful collaboration and sharing the lab life with me: Santi, Dolors, Jordi M., Alberto, Daniel, Pau, Miguel, Irati, Fan, Enric, Shauna, Pablo, Doga, and Evangelia.

It is a great pleasure to acknowledge the support and help coming from the technicians from the Microscopy Service, X-ray Diffraction, ICMAB, University of Barcelona and ICN2 for their assistance in SEM, XRD and cell experiments.

Thanks to the grant from the China Scholarship Council (CSC). Without that, I would not have had the chance to pursue my PhD in UAB.

I would like to thank my Chinese friends Xiaodan, Zhihai, Jinrong, Mengjie, Weijie and Changyong for their help and support. I do not feel lonely with their companion.

Thanks to my parents and my sister for their wise counsel and sympathetic ear. You are always there for me.

Finally, I would like to thank the girl in my dreams even though I do not know where you are now. I know I will meet you eventually if I keep going beyond myself. It is not easy to say OK when you are studying abroad, but this persistance will make me close to you.

Yuping Feng

Abstract

This Thesis dissertation covers different synthetic approaches to obtain Fe-based alloys to be used for biomedical and environmental applications. Special emphasis has been placed to design a proper composition and to study the morphology and structural properties to tailor both the mechanical and magnetic properties of the resulting materials.

Firstly, ferromagnetic Fe-10Mn6Si1Pd (wt.%) and shape memory, paramagnetic Fe-30Mn6Si1Pd (wt.%) compact alloys were prepared by arc-melting followed by copper mold suction casting. The evolution of microstructure, mechanical and magnetic properties, as well as the assessment of degradation, cytotoxicity and cell proliferation in Hank's solution as a function of the immersion time were systermatically studied.

With the aim to improve the biocompatibility of the Fe-10Mn6Si1Pd alloy, calcium phosphate coatings (CaP) (i.e., brushite and hydroxyapatite) were electrodeposited on the alloy by pulsed current electrodeposition. Due to porous structures resulting from needle-, rod- or plate-like morphologies, the measured Young's modulus and hardness of these coatings were lower than those of fully-dense CaP layers with analogous compositions.

Then, to increase the degradation rate and to reduce the Young's modulus of the fully bulk alloys, porous Fe-30Mn6Si1Pd (wt.%) alloys were prepared by a simple press and sinter process from ball-milled Fe, Mn, Si and Pd powders blended with 10 wt.%, 20 wt.% and 40 wt.% NaCl. Remarkably, the reduced Young's modulus of all the porous alloys reached values close to 20 GPa after long-term immersion, a value which is close to the Young's modulus of human bones (3–27 GPa), hence favoring good biomechanical compatibility between an eventual implant and the neighboring bone tissue.

Meanwhile, open cell Fe and Fe-Mn oxides foams were prepared by the replication method using porous polyurethane templates. The magnetic response of the foams, from virtually non-magnetic to ferrimagnetic, could be tailored by controllably adjusting the Mn content as well as the N_2 flow rate. Still dealing with magnetic properties, femtosecond pulsed laser irradiation was used to create periodic magnetic patterns at the surface of a non-ferromagnetic amorphous Fe-based alloy.

Finally, a nanoporous Fe-rich alloy was prepared by selective dissolution of melt-spun $Fe_{43.5}Cu_{56.5}$ ribbons. The nanoporous ribbons were found to be an excellent heterogeneous Fenton catalyst towards the degradation of methyl orange in aqueous solution.

Resum

Aquesta tesi doctoral comprèn la síntesi d'aliatges basats en ferro mitjançant diversos mètodes de fabricació. Aquests aliatges s'han dissenyat amb la intenció de ser utilitzats en biomedicina o en aplicacions mediambientals. S'ha donat especial èmfasi a dissenyar una composició adequada i a estudiar la morfologia i les propietats estructurals per tal d'optimitzar tant les propietats mecàniques com les propietats magnètiques dels materials resultants.

En primer lloc es va utilitzar la tècnica de fusió per arc i colada per succió amb motlle de coure per fabricar dos aliatges densos: un aliatge ferromagnètic amb composició en pes Fe-10Mn6Si1Pd i un aliatge paramagnètic amb memòria de forma amb composició en pes Fe-30Mn6Si1Pd. L'evolució de la microestructura, les propietats mecàniques i magnètiques, així com també la degradació, la citotoxicitat i la proliferació de cèl·lules en solució Hanks es van estudiar de forma sistemática en funció del temps d'immersió.

Per tal de millorar la biocompatibilitat de l'aliatge Fe-10Mn6Si1Pd, aquest aliatge es va recobrir amb fosfat de calci (brushita o hidroxilapatita) mitjançant la tècnica d'electrodeposició per corrent polsant. A conseqüència de la morfologia porosa d'aquests recobriments (per exemple: en forma d'agulles, cilindres o plaques), el mòdul de Young i la duresa mesurades foren inferiors als valors obtinguts en recobriments anàlegs no porosos.

Seguidament, amb l'objectiu d'incrementar la velocitat de degradació i reduir el mòdul de Young d'aquests aliatges compactes, es van fabricar aliatges porosos de Fe-30Mn6Si1Pd mitjançant un procés de premsa i sinterització de Fe, Si, Mn i Pd en pols prèviament mòlta i barrejada amb un 10, un 20 o un 40% en pes de NaCl en un molí de boles. Cal destacar, que després de submergir els aliatges porosos durant un període llarg de temps, el mòdul de Young reduït que es va mesurar en tots ells va ser d'uns 20 GPa (essent aquest valor similar al mòdul de Young de l'os humà, entre 3-27 GPa). Aquest fet afavoriria una bona compatibilitat biomecànica entre l'implant i el teixit ossi veí.

Per altra banda, es van fabricar escumes de Fe i Fe-Mn de cèl·la oberta utilitzant matrius de poliuretà poroses pel mètode de rèplica. Es va observar que la resposta magnètica d'aquestes escumes, des de pràcticament no magnètica a ferrimagnètica, es podia controlar ajustant el contingut de Mn i el flux de N_2. També, en el marc de propietats magnètiques, es va utilitzar la tècnica d'irradiació amb làser polsat de femtosegon per crear patrons magnètics periòdics a la superfície d'un aliatge amorf no ferromagnètic basat en Fe.

Finalment, es va preparar un aliatge nanoporós ric en Fe per dissolució selectiva de cintes de $Fe_{43.5}Cu_{56.5}$ fabricades per tornejat en estat de fusió. Es va observar que els materials nanoporosos eren un excel·lent catalitzador heterogeni de la reacció de Fenton per la degradació del taronja de metil en solució aquosa.

Table of contents

Table of contents

Glossary

- Atomic force microscopy (AFM)
- Berkovich Hardness (H_B)
- Biodegradable metals (BMs)
- Body-centered cubic (BCC)
- Bulk metallic glasses (BMGs)
- Calcium phosphates (CaP)
- Carbon nanotubes (CNT)
- Corrosion current (I_{corr})
- Corrosion potential (E_{corr})
- Direct current (DC)
- Dulbecco's Modified Eagle Medium (DMEM)
- Energy dispersive X-ray (EDX)
- Face-centered cubic (FCC)
- Femtosecond pulsed laser irradiation (FSPLI)
- Field emission scanning electron microscopy (FESEM)
- Foetal Bovine Serum (FBS)
- Hexagonal close-packed (HCP)
- Hemolysis ratio (HR)
- Hydroxyapatite (HAp)
- Inductively coupled plasma (ICP)
- Liquid metal dealloying (LMD)
- Magnetic force microscopy (MFM)
- Magnetic resonance imaging (MRI)
- Methyl orange (MO)
- Nanoparticles (NPs)
- Nuclear magnetic resonance (NMR)
- Open circuit potential (OCP)
- Optical density (OD)
- Phosphate buffered saline (PBS)

Glossary

- Poly(lactic-co-glycolic acid) (PLGA)
- Polyurethane (PU)
- Powder metallurgy (PM)
- Quantitative nanomechanical (QNM)
- Rare earth (RE)
- Reduced Young’s modulus (E_r)
- Scanning electron microscopy (SEM)
- Selective laser melting (SLM)
- Shape memory alloys (SMAs)
- Solid-gas eutectic solidification (Gasar)
- Ultra-Micro-Indentation System (UMIS)
- Ultraviolet (UV)
- Vibrating sample magnetometer (VSM)
- X-ray diffraction (XRD)
- X-ray photoelectron spectroscopy (XPS)
- Zero-valence iron (ZVI)

1. Introduction

Chapter 1: Introduction

Chapter 1: Introduction

1.1 State-of-the-art of Fe-based alloys: Fe as a structural material

Iron is one of the most common chemical elements on Earth, with symbol Fe, forming around 5% of the Earth's crust. The atomic number of iron is 26 and the atomic weight is 55.847. Iron is a transition metal which belongs to the group 8 in the periodic table, along with Ruthenium (Ru), Osmium (Os) and Hassium (Hs). Its ubiquity, working qualities and tenacity make iron one of the most valuable metals. Pure iron is a silvery white metal with a lustrous surface. Thanks to its malleable and ductile nature, it can be easily molded into different shapes without breaking or cracking. Iron also has good heat and electrical conductivity, directly affecting the quality of our lives. Iron ore is one of the first ores that humans have exploited for making tools since ancient times, playing a major role in human history. Iron melts at 1538 °C, and boils at 3070 °C [1]. The density of iron is 7.874 g/cm^3 and its Young's and shear moduli at room temperature are 200 GPa and 78 GPa, respectively. Elemental or pure iron is difficult to be found in nature as its chemical reactivity is very high and it corrodes rapidly, forming an oxide layer on the surface, especially at elevated temperatures or in moist air. The two most common oxidation forms of iron are Fe(II) and Fe(III), in which the metal loses two or three of its electrons, although iron was found to exist in other oxidation forms (from +2 to +6).

Pure Fe is relatively soft, but alloying Fe with a certain proportion of other elements, for instance, carbon (steel) can significantly harden and strengthen it. Steels and iron-based alloys are about 95% of the total metal alloys that are being manufactured. Such a high production and extensive use is achieved, not only by the abundant and easy-exploitation of iron-bearing rocks, but also because of the low-cost processing and the great range of desirable properties that it can offer.

There are three allotropes of iron known as “ferrites” at atmospheric pressure: δ-iron allotrope, body-centered (BCC) crystal structure; γ-iron allotrope, face-centered cubic (FCC) structure (austenite); α-iron allotrope, BCC structure (ferrite) (Figure 1.1). Figure 1.2 shows the low-pressure phase diagram of pure iron with regions belonging to the above-mentioned crystal structures. However, at very high pressure (10 GPa), although not depicted in the diagram, a fourth form exists, called ε-iron, which has the hexagonal close-packed (HCP) crystal structure. Besides crystal structure evolution, the most important property of iron is the Curie temperature (770 °C), below which a positive exchange interaction exists between the magnetic moments of neighboring atoms and iron becomes ferromagnetic, even though there is no change in the crystalline structure.

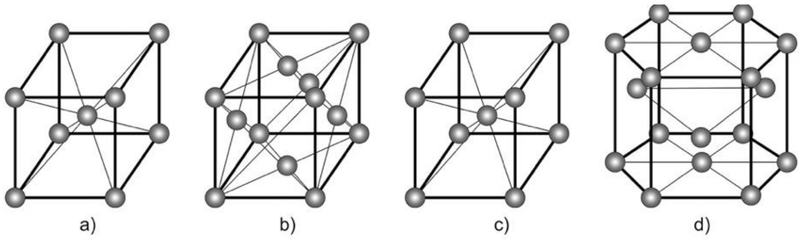

Figure 1.1: Allotropes of iron: a) alpha (α) iron, b) gamma (γ) iron, c) delta (δ) iron and d) epsilon (ε) iron.

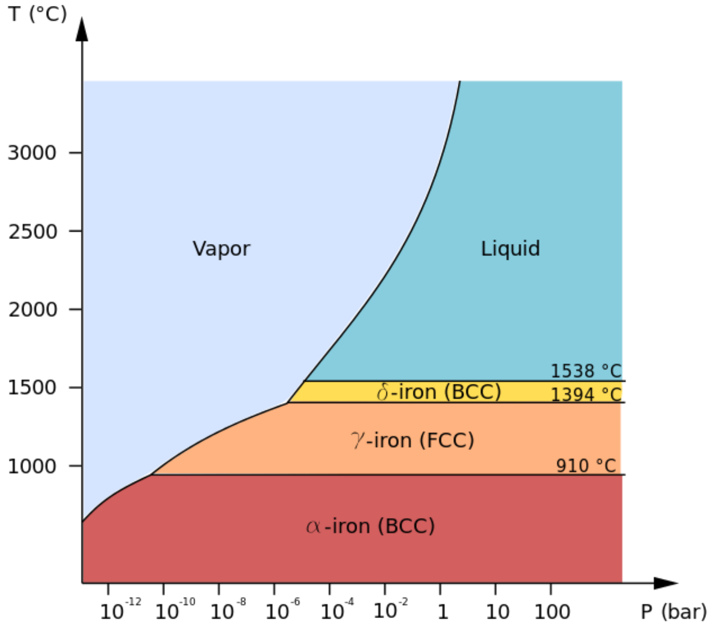

Figure 1.2: Phase diagram sketch of pure iron at low pressure.

Iron plays a very important role in humans because it is used in the production of complexes with molecular oxygen in myoglobin and hemoglobin; these two substances are vital oxygen-transport proteins within the body; iron is also one of the indispensable components of the human metabolism. In addition, it is one of the most important trace elements in the body and it commonly exists in two primary oxidation states: Fe^{2+} ions and Fe^{3+} ions. The daily intake of iron for a human of average height is 10-20 mg, however, less than 10% is absorbed. Iron is widely distributed throughout the human body in myoglobin, hemoglobin, bone marrow, tissues, muscles, hemosiderin, ferritin, and through a number of enzymes which participate in different vital cell processes (e.g. oxidase, catalase, peroxidase, cytochromes, aconitase, nitric oxide synthases and ribonucleotide reductase). Iron is also an indispensable element for brain development; for example, a lack of iron in children results in a lower learning ability.

Because Fe is one of the most abundant elements in nature and because of its low-cost processing, Fe-based materials are widely used in engineering applications. In fact, steel is the most important engineering material in the world. Fe-based superalloy materials, such as Fe-Ni, were developed to design materials with higher tensile ductility, lower creep extension, larger resistance to crack propagation and high-temperature applications [2]. Fe-based shape memory alloys (SMAs), such as Fe–Mn–Si alloys, are promising candidates to be employed as prestressing tendons in civil engineering structures [3]. Barium and strontium ferrite magnets with high coervicity are the main permanent magnets resource and are widely used in magnetic recording media [4]. Beyond these conventional applications, Fe has started to be exploited in some novel applications, like in superconductors, biodegradable materials, bulk amorphous soft magnetic materials or catalysts. It is the aim of this Thesis to explore novel applications for Fe-based materials.

1.2 Beyond structural applications: biomedical applications

With the increasing expectations of living standards and the recent development of advanced theoretical and experimental setups, novel biomaterials have received widespread attention and have achieved a rapid development to improve the quality of life and prolong life cycle significantly.

Conventional biomaterials have been used to treat diseases or injuries since thousands of years ago. For example, coral or wood were used as dental implants and fabric was used for sutures in early times [5]. Up to date, most of the materials used to manufacture medical implants are metals, polymers and ceramics. Moreover, increasing attention is being paid to hybrid materials, alloys, composites and nanomaterials with improved properties. Among the multifarious biomaterials, metallic ones have the longest history because metals show excellent wear resistance, higher toughness and good ductility compared with other non-metallic materials [6].

The first metallic biomaterials used in clinical practice were permanent implants. Late on the 18th century, pure Fe, Ag, Au and Pt were cut and machined as wires and pins to treat bone fractures [6]. Nowadays, stainless steel, Ti alloys and Co-Cr alloys with improved corrosion resistance are widely used materials for orthopedic load-bearing implant and fixation devices such as dental implants, bone plates and screws, orthopedic wires, hip or knee prosthesis, and coronary stents [6, 7].

Corrosion is a well-known failure issue in metallurgy. Hence, resistance to corrosion must be taken into account when designing new permanent metallic implants as corrosion products are considered to have detrimental consequences for the surrounding tissue. While corrosion shortens the lifecycle of permanent implants, it has been observed that corrosion, in a controlled manner, is desirable for the degradation of biodegradable implants (e.g. Mg-based or Fe-based alloys) [6]. Temporary, biodegradable materials have revolutionized the field of biomedical implants by combining engineering and medical requirements for implants [6]. Hence, the definition of biomaterials has changed from merely mechanical engineering replacement devices towards new biological solutions, allowing biodegradable materials to become promising candidates for regenerative medicine [8]. In 1878, Edward C. Huse already used Mg wires as ligatures for bleeding vessels and a lower corrosion rate of Mg *in vivo* was observed [9]. Degradable biomaterials should actively interact with the tissue and promote healing, instead of passively replacing the missing tissue (permanent bone substitutes) or support the vessel (permanent coronary stents). The essence of the biodegradable medical implant concept lies in the fact that in many cases (e.g. stents), the implant needs to stay in the body only during the healing process, to provide, for instance, mechanical strength and to support the life of the surrounding tissue. Once the healing process is over, the implant should gradually disappear without leaving harmful elements behind [10]. Besides vascular stents and orthopedic implants, biodegradable materials are also exploited as drug reservoirs.

Zheng et al. [11] provided a most accurate definition of biodegradable metals (BMs): "Metals are expected to corrode gradually in *vivo*, with an appropriate host response elicited by released corrosion products, then dissolve completely upon fulfilling the mission to assist with tissue healing with no implant residues". Therefore, the major component that constitutes the whole metallic material (alloying elements or composite elements) must be free of harmful effects on the living tissue during the degradation process, allowing their metabolization within the body, and demonstrating suitable degradation rates [11, 12].

Until now, Mg-based BMs [13-17] (pure Mg, Mg–Zn, Mg–Ca, Mg–Sr, Mg-Mn, Mg–RE (rare earth) alloys, etc.) and Fe-based BMs [18-47] (pure Fe, Fe–Mn, Fe-W, Fe-P alloys, etc.) are recognized as the two main families of BMs. Pure metals, alloys, and composites based on Fe and Mg are investigated from different aspects in order to make them suitable for clinical applications as degradable implants. As previously mentioned, an important requirement for BMs is to achieve controlled corrosion rates and, thus, provide a predictable and controlled way of degradation. During the last decade, many investigations have focused on testing the basic properties (i.e., structure, morphology, biocompatibility, mechanical properties, magnetic behavior) and also the fabrication technologies for both, the material and the implant itself, paying attention to corrosion related aspects in order to find optimally suited BMs [10].

Although other systems are arising as promising candidates to be used as BMs, such as Zn-based BMs [48, 49], Ca-based bulk metallic glasses (BMGs) [17, 50] and Sr-based BMGs [51, 52], Fe- and Mg-based systems still remain the most widely explored BMs. Mg-based BMs are currently at vanguard's research and a few patented coronary stent solutions have been put forward. Mg and its alloys are free from toxic elements, exhibit fast biodegradability, and a Young's modulus close to that of the human bone. However, the exceedingly high degradation rates of Mg alloys may limit their use in certain applications where the implant needs to stay in the body for at least a specific period of time. Furthermore, the accompanying considerable amounts of released hydrogen can impede a good connectivity between osteocytes and the alloy. Also, for some applications, the strength and ductility of Mg-alloys are not good enough to hold the body's weight. To overcome these issues, Fe-based BMs arose as promising alternative candidates. As mentioned in section 1.1, recognized advantages of Fe-based materials are: low cost, wide range of available alloying elements and the widest possible presence of production plants for iron processing throughout the world. Up to date, the main disadvantage of Fe-based alloys to be used as biodegradable metallic materials is their exceedingly low degradation rate, which hinders their applicability in real clinical trials. The requirements of Fe-based biodegradable materials can be summarized as follows:

- Good biocompatibility and non-cytotoxicity
- Appropriate degradation rate
- Low Young's modulus
- Good ductility
- Non-magnetic behavior (to allow for magnetic imaging technologies)

Nowadays, many research activities are devoted to the development of Fe-based degradable implants that fulfill these requirements (i.e. new fabrication methods, novel structure design, addition of alloying elements, etc.).

1.2.1 Novel iron-based biodegradable metallic materials

The first pure iron stent was produced in 2001 and implanted into aorta of New Zealand white rabbits. It was not cytotoxic and it did not cause any inflammatory response or other side effects [53]. However, preliminary animal tests revealed that pure iron suffered from too low biodegradation rates in *vivo*, which were even considered similar to that of permanent steel stents [54]. A more serious limitation was that pure Fe is ferromagnetic, thus precluding their use in specific applications where magnetic resonance imaging (MRI) analysis or nuclear magnetic resonance (NMR) is required to monitor the patient’s recovery after surgery. Hence, new non-magnetic Fe-based alloy compositions with improved degradation rates to be used as biodegradable stents were designed via the addition of alloying elements [22, 27, 30, 31, 33, 36, 40-42, 55-58]. In fact, many research studies [22, 27, 30, 31, 33, 36, 40-42, 55-58] are currently focused on the study of the effects of alloying elements on the corrosion rate, mechanical properties, biocompatibility and ferromagnetism.

Some of the most commonly used alloying elements are listed below:

A: Manganese

Hermawan et al. [47] first reported a new class of Fe-35Mn alloy produced by powder metallurgy (PM) to be used as degradable metallic stent. It shows paramagnetic behavior and thus, provides an excellent MRI compatibility. It also has low inhibition to fibroblast cells, indicating that the alloy is biocompatible [47, 59]. In addition, Mn is a trace essential element in many enzymatic reactions [47]. Liu et al. [25] also pointed out that the addition of Mn can increase the strength of pure Fe. Furthermore, the addition of Mn within the solubility limit of Fe reduces the standard electrode potential of Fe and thus make it more susceptible to corrosion [22].

B: Palladium

Schinhammer et al. [22] proposed the Fe–Mn–Pd system as a good candidate for stent applications [31]. It is believed that the addition of noble alloying elements, such as Pd, can generate homogenously distributed small (< 10 nm in size) Pd-rich precipitates that can act as cathodic sites to induce microgalvanic corrosion. Furthermore, the small noble intermetallic (Fe,Mn)Pd precipitates exhibit a very low diffusion coefficient, thus improving the mechanical properties of the system [31, 33].

C: Silicon

Alternatively, Liu et al. [25] pointed out that the addition of 6 wt.% of Si to Fe-30Mn alloy rendered a material with shape memory effect. Furthermore, they found out that the Fe-Mn-Si system exhibits better corrosion performance than the Si-free Fe-Mn analogue. No harmful effects on cells were detected [25].

D: Carbon

Xu et al. [60] produced a novel as-forged Fe–30Mn–1C alloy by vacuum melting, which showed improved mechanical properties and enhanced degradation rate compared with Fe-30Mn alloy. C addition also lowers the magnetic susceptibility of the alloy making it more suitable for MRI [60]. Wegener et al. [29] also observed slightly larger corrosion rates with carbon addition. However, some authors reported opposite results; Mazou et al. [57] showed that the Fe-20Mn-1.2C alloy exhibited lower corrosion rate than pure iron because of the formation of an adhesive degradation layer which prevented the contact between the electrolyte and the alloy.

E: Phosphorous

Low phosphorous content in iron is beneficial for rapid densification and can increase the sintering density, which, in turn improves the mechanical properties, as shown by Wegener et al. [29]. The authors also showed that low phosphorous contents did not decrease the corrosion rate or cell proliferation compared with pure iron [29]. Further addition of phosphorus above the solubility limit is, however, not recommended as this would cause material embrittlement.

1.2.2 Fabrication methods for iron-based biodegradable metallic materials

There are several production technologies that can be efficiently used to fabricate iron-based materials. The main goal in the production of Fe-based implants is to increase the corrosion rate while providing sufficient mechanical strength and biocompatibility. Among the most widely used techniques, one can list the following:

A: Powder metallurgy

PM is a powerful technique that allows tailoring the corrosion properties while maintaining other necessary material properties. It can deliver fully dense or porous materials almost without impurities, except those predefined by material's design. For instance, Hermawan, et al. [36, 42, 47] produced a series of iron-based alloys containing 20–35 wt.% of manganese; they found out that the alloys with 20 and 25 wt.% of Mn showed the highest degradation rates. This technique has also been used to fabricate porous structural metals or alloys for bone implants by the addition of a porogen (e.g. NH_4HCO_3) to the raw powders [61], which, in turn, sublimates during a thermal treatment or dissolves, leaving numerous pores beneath.

B: Electroforming

Electroforming is a suitable technique to produce free-standing Fe-based thick films. It renders polycrystalline metals with grain sizes much smaller than those of bulk counterparts produced by other available production techniques. For instance, Moravej et al. [6, 20, 21] prepared pure Fe films by electroforming technology. These films exhibited a faster corrosion rate than pure Fe produced by casting and thermomechanical treatment in both, static immersion and dynamic degradation tests. This was attributed to a more uniform degradation mechanism. High yield strength (360 MPa) and tensile strength (423 MPa) were also reported [20]; these values are higher than those of pure iron produced by casting method.

C: 3D printing

3D printing is a cost-efficient and widely available technology to prepare complex porous structural materials. Chou et al [18] prepared Fe-30Mn biodegradable metallic scaffolds by inkjet 3D printing with similar mechanical properties to those of natural bone. In addition, enhanced biodegradation rates and good in *vitro* cytocompatibility make 3D printed Fe–Mn scaffolds good candidates for craniofacial applications. Figure 1.3 shows typical morphologies of 3D printed Fe-Mn and Fe-Mn-1Ca alloys.

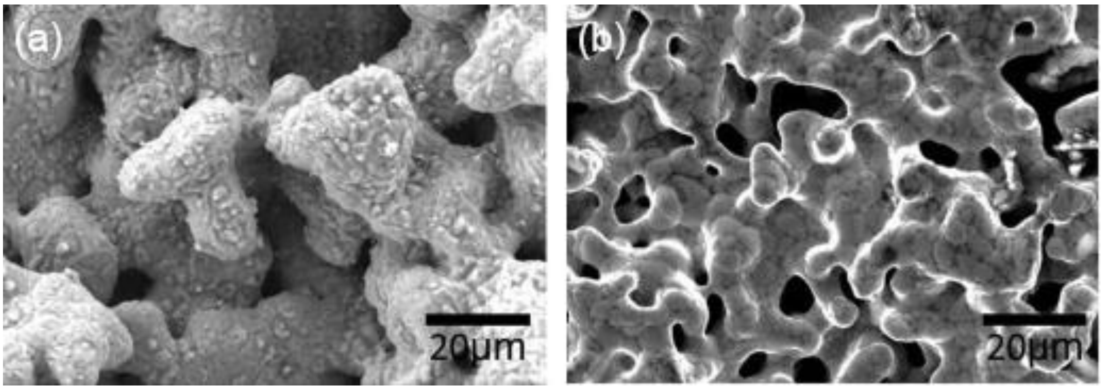

Figure 1.3: Scanning electron microscopy images of 3D printed (a) Fe-Mn and (b) Fe-Mn-1Ca samples [35].

1.2.3 Novel structure design for iron-based biodegradable metallic materials

Novel structural iron-based BMs with enhanced properties have attracted increasing interest to be used in a wide range of medical device applications. Some of the new paths that researchers are following to obtain improved properties are: the design of a composite structure, the design of porous materials, and to coat Fe-based implants with biocompatible materials:

A. Composite structures

In order to increase the degradation rate of pure Fe, extensive research has been devoted to the development of various Fe-based composites, such as Fe–Pd and Fe–Pt composites [26], Fe–W, Fe–CNT (carbon nanotubes) [24], and Fe–Fe_2O_3 [23].

Huang et al. [26] used spark plasma sintering to produce Fe-5wt.%Pd and Fe-5wt.%Pt composites and achieved smaller grain sizes and better mechanical characteristics compared to as-cast pure iron. Both Pd and Pt elements increased the corrosion rate by approximately 2.73 times in comparison with pure iron. Hemolysis was lower than the tolerated level of 5% for both composites. Cheng et al. [23] prepared a series of Fe–Fe_2O_3 composites with different weight percentages of Fe_2O_3 (2, 5, 10 and 50 wt.%) by spark plasma sintering and obtained larger corrosion rates in comparison with pure iron. The final composite structure consisted of α-Fe and FeO instead of Fe_2O_3. Fe–

5wt.%Fe_2O_3 is considered as the best option as biodegradable material because of its good combination of mechanical and biocompatible performance.

B. Porous structures

The introduction of porosity is an effective way to lower the Young's modulus of the implant to values closer to that of the human bone (3-25 GPa) [62], as Young's modulus (and the yield stress) are both proportional to the relative density of the material [63]. Namely, both hardness and Young's modulus progressively decrease with the increase of porosity. Moreover, porosity increases the overall available surface area of the material to the corrosive environment, which might enhance the degradation process. For bone tissue engineered scaffolds, porosity is a key factor that enables the possibility of surrounding cells to proliferate through the pores by allowing tissue ingrowth and the transportation of body fluids. Porous metallic materials are also promising platforms for drug delivery applications [64]. For instance, Wegener et al. [29] used PM to prepare porous Fe-based alloys, which showed enhanced degradation rate and better biocompatibility properties while maintaining the mechanical properties.

C. Coatings

Another means to increase the corrosion rate of Fe is to cover bulk iron with suitable coatings [46, 65-67]. For example, the corrosion rate of a composite consisting of micro-patterned gold disk arrays deposited by sputtering on Fe was 4 times higher than the corrosion rate of pure iron [66] because the corrosion mechanism turned into macroscopically uniform. Recently, a new poly(lactic-co-glycolic acid) (PLGA)-coated porous iron alloy was prepared with the aim to accelerate the degradation process of iron while maintaining its good biocompatibility, even during the most active degradation period [28].

In turn, the development of ceramic coatings such as hydroxyapatite (HAp) or other various forms of calcium phosphates (CaP) on metallic implants has been documented to increase their biocompatibility as the bioactive coating can form a direct chemical bond with the bone [68, 69].

1.3 Beyond structural applications: environmental applications

On the Earth's surface, water seems to be one of the most widespread natural resources, but unfortunately only 2.53% of the total is freshwater and only about one third of this freshwater is available for human consumption [70-72]. According to the report from World Health Organization, over 1.8 billion people use contaminated drinking-water sources. With the enormous growth in industrial and agricultural activities, continuous contamination of freshwater resources by a variety of organic and inorganic pollutants has become one of the major environmental threats to human health and ecosystems in general [73, 74]. Over the last few decades, abundant sorts of physical, chemical, and biological treatments of wastewater and drinking water have been introduced to remove non-degradable organic compounds from industrial wastewater. However, these existing technologies of wastewater treatment are not efficient enough to completely remove the emerging contaminants and meet the increasing strictest water quality standards [75]. For instance, physical processes such as liquid−liquid extraction or ion-exchange can remove the contaminant by converting the pollutants to other compounds while producing a highly concentrated sludge [76, 77], which are ineffective for pollutants that are not easily absorbable or volatile. Membrane filtration, which can remove abundant contaminants, enables the possibility of using seawater, brackish water and wastewater; however, it requires very high water pressure, which in turn causes large energy power consumption [75]. Activated carbon adsorption processes are also very costly [78]. Ozone and hypochlorite oxidation processes are efficient, but the costly equipment and secondary pollution produced by residual chlorine make them undesirable [79]. In fact, many of these methods simply convert the pollutants to other compounds, rather than actually eliminating them [80]. Remarkably, some efficient and powerful methods comprising advanced nanotechnology concepts have been proved as promising wastewater remediation approaches since they can induce almost complete mineralization of a wide range of organic pollutants [81]. Among the various nanotechnologies available, they can be divided into three main categories considering the nature of the nanomaterials involved: nano-adsorption technology, nano-catalysis, and nano-membranes.

Iron or ferric oxides, which are commonly used in the field of nano-adsorption and nano-catalysis, are extensively utilized for hazardous pollutants removal from wastewater owing to their low cost, minimum environmental fingerprint and absence of secondary pollutants.

1.3.1 Iron based nanoparticles (Fe_3O_4) as nano-adsorbents

Ferric oxides (Fe_3O_4) [82], as well as manganese oxides [83], magnesium oxides [84], zinc oxides [85] and titanium oxides [86] have specific affinity to absorb impurities. They are considered eco-friendly materials for the adsorption of noxious metals with less chance of secondary contamination [87, 88]. The adsorption rate and factors affecting the removal efficiency of metal ions on Fe_3O_4 magnetic nanoparticles (NPs) can be found in the literature [82, 89, 90]. The adsorption efficiency of Ni^{2+}, Cu^{2+} and Cr^{6+} ions by Fe_3O_4 NPs is influenced by temperature, pH, surface functionality, adsorbent dose and incubation time. These parameters determine the efficiency of Fe_3O_4 NPs to adsorb poisonous metal ions selectively [91]. For instance, approximately 100% adsorption rate of Ni^{2+}, Cu^{2+}, Cr^{3+}, Co^{2+}, Cd^{2+} and Pb^{2+} metal ions from wastewater was monitored in a solution with pH>8 containing surface-functionalized (carboxyl-, amine- and thiol-) Fe_3O_4 NPs. Compared with bare Fe_3O_4 magnetic NPs, surface-functionalized Fe_3O_4 NPs [82, 92-97] show significantly improved adsorption efficiency. Moreover, CNTs modified with iron oxide [98, 99] also show significantly improved performance for heavy metals removal from wastewater.

1.3.2 Iron based nano-catalysts

Nano-catalysts like iron-based Fenton catalysts [100], photocatalysts [101] and electrocatalysts [101] can be used for water remediation because they can promote chemical oxidation of antimicrobial actions [102] and organic pollutants [103].

Superparamagnetic γ-Fe_2O_3 NPs are considered as one of the most desirable materials as reusable catalysts due to their distinct catalytic (large surface area results in high catalyst loading capacity), magnetic properties, low-cost preparation and environmental-friendly character [101]. Another major advantage of the use of γ-Fe_2O_3 catalysts is that they can be recovered at the end of the reaction by simple magnetic decantation [104], which is much more convenient than the traditional methods like cross-flow filtration and centrifugation. Furthermore, the magnetic properties of the γ-Fe_2O_3 catalysts particles are stable enough to maintain their properties even in extremely acidic or corrosive chemical environments.

Fenton reactions (i.e., iron-catalyzed hydrogen peroxide) can either oxidize the contaminants to smaller organic molecules or transform them into water, carbon dioxide, or salts [105-110]. Besides water remediation, Fenton reactions are also of interest in biological applications because they involve the creation of free radicals by chemicals that are present in bodily fluids. Some additional advantages of Fenton reactions are their high efficiency, simplicity to destroy the contaminants, and the non-requirement of sophisticated equipment [111]. Moreover, the reaction takes place under ambient conditions [112]. For these reasons, homogeneous Fenton catalysts (in which Fe cations are directly dissolved in liquid media) have been widely investigated and are now being considered to be used in wastewater treatment [113]. As an alternative to homogeneous Fenton, some attempts have been made to develop “heterogeneous” Fenton catalysts, that is, solid materials that are immersed, but not dissolved, in the media while providing a high catalytic activity. In principle, some of the limitations encountered by a homogeneous process might be overcome by heterogeneous Fenton oxidation processes [114, 115]. Namely, it has been reported that heterogeneous Fenton oxidation exhibits lower activation free energy than homogeneous Fenton reactions [116]. Furthermore, during heterogeneous Fenton reactions, high amounts of surface active sites for H_2O_2 decomposition and formation of hydroxyl radicals take place, sometimes inducing higher removal efficiency compared to homogeneous Fenton processes [117]. Heterogeneous Fenton catalysts can be prepared by incorporating Fe ions, zero-valence iron (ZVI), or Fe oxide phases (e.g., in the form of NPs) into porous scaffolds that act as support materials (e.g., zeolites, nafion, clay, or activated carbon) [118-120]. Figure 1.4 shows a schematic drawing of a heterogeneous Fenton process. In Fenton-like heterogeneous reactions, catalysis originates at the surface of the catalyst. Hence, the adsorption of H_2O_2 and other reactants at the catalyst surface plays an important role. In the presence of H_2O_2, Fe^0 oxidizes to Fe^{2+} by the transfer of two electrons, as shown in eq 1:

$$Fe^0 + H_2O_2 + 2H^+ \rightarrow Fe^{2+} + 2H_2O \qquad (1)$$

In the classical Fenton reaction, the production cycle of hydroxyl radicals can be represented as follows:

$$Fe^{2+} + H_2O_2 \rightarrow Fe^{3+} + OH^{\bullet} + OH^- \qquad (2)$$

$$Fe^{3+} + H_2O_2 \rightarrow Fe^{2+} + OOH^{\bullet} + H^+ \qquad (3)$$

An example of the use of nanoporous Fe ribbons (produced by dealloying) as heterogeneous Fenton catalysts for the decolorization of a dye solution is shown in Figure 1.4. The sorption rate of the organic contaminant can be one of the main controlling factors during the whole catalytic oxidation reaction.

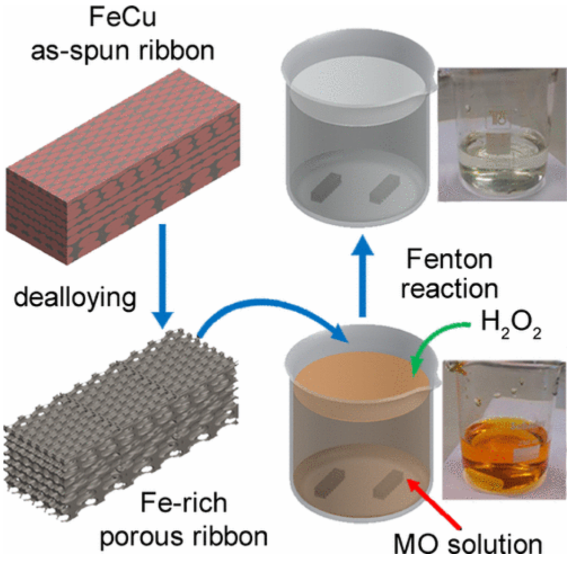

Figure 1.4: Schematic drawing of the dealloying process to produce Fe-rich nanoporous ribbons from FeCu alloy ribbons and the degradation of methyl orange (MO) by taking advantage of the Fenton reaction over the nanoporous Fe ribbons [74].

1.4 Approaches to create porous structural metals (cellular metallic materials)

Porous structural metals are solid forms of metals or alloys distributed by different kinds of interconnected or non-interconnected pores (holes): apertures, channels or cavities. Depending on their pore size, they can be classified into two groups: macrocellular porous metals and nanoporous metal materials. The morphology of the macrocellular metal foams consists of micro-scale holes embedded in a dense metal matrix; they exhibit relatively low density and high surface area. Even though the terms porous (structural) metal or cellular metals are idiomatic expressions referring to metals containing any kinds of pores, it is useful to classify them as follows:

1. **Porous (Structural) Metal:** The most general expression, which means that a metal has a large volume of pores. A sintered porous bronze metal is presented in Figure 1.5 (a).

2. **Cellular Metal:** Similar term to “porous metal” but in this case individual cells or voids are all separated from each other. This means that cellular metals are formed by individual cells or voids with solid metal cell boundaries. Figure 1.5 (b) shows a typical cellular metal with solid metallic boundaries to separate the pores. On the contrary, the porous material presented in Figure 1.5 (a) cannot be considered a cellular metal because it has no pore walls.

3. **Metal(lic) Foam:** Foams are homogenous dispersions of gaseous cells or voids which are closed, round and separated by thin metal boundaries in either a liquid or a solid state [121]. Figure 1.5 (c) shows an aluminum foam with high porosity. Originally, a metallic foam is referred to a liquid metal foam; however, solid metal foam with the same morphology forms after liquid solidification.

4. **Metal Sponge:** Highly porous materials with interconnected voids. Figure 1.5 (d) shows a typical nickel sponge with interconnected pores.

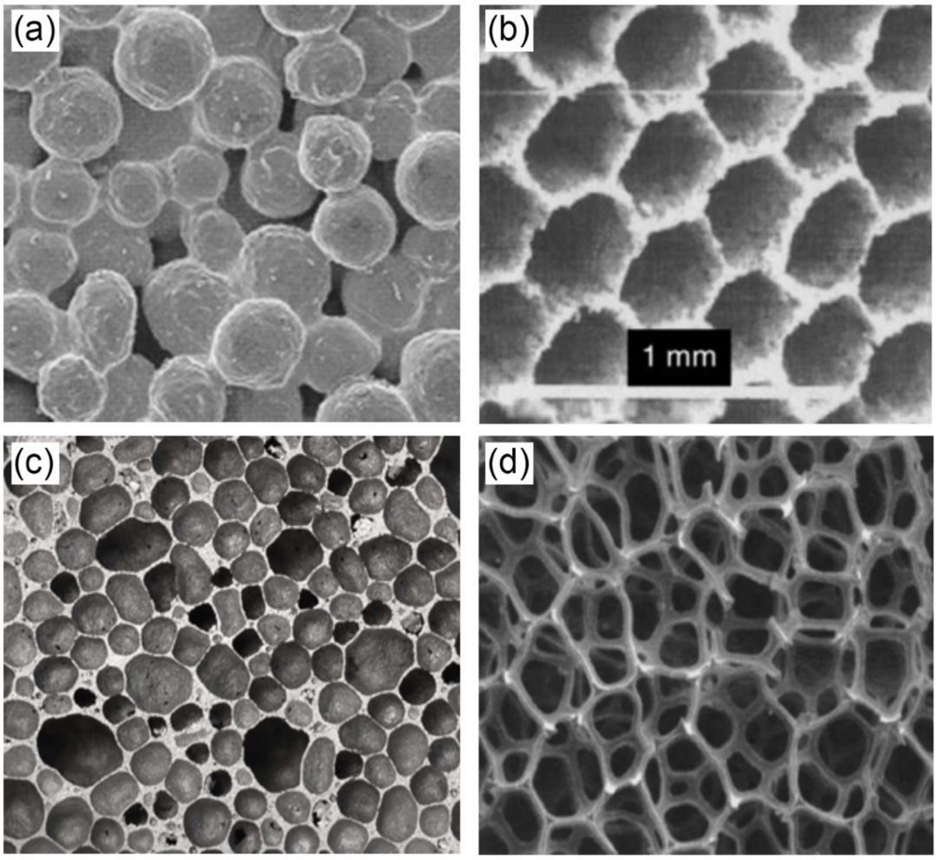

Figure 1.5: Examples of various types of porous metals: (a) porous metal, (b) cellular metal, (c) metallic foam and (d) metal sponge.

All these definitions are not mutually exclusive. In this work, we will use the terms porous (structural) metals or cellular metals to refer to all metals containing any kinds of pores.

Cellular metallic materials combine properties of metals, such as good thermal and electric conductivity, excellent mechanical properties and good catalytic activity, with specific features of the porous structural architecture, like high specific surface area, low density, controllable pore size and relatively narrow pore size distribution. These characteristics of cellular metallic materials have been gaining rapid attention in structural applications like aerospace industry, biomedical industry, machine construction and in functional applications like catalysis, water purification, filtration, battery electrodes, etc.

There are many methods available to produce cellular metallic materials. These methods can be divided into two groups: solid metals in powder form or liquid metals.

1.4.1 Cellular metallic materials produced from solid metals in powder form

A porous metal or metal foam can be produced if the metal is pressed and sintered using conventional powder metallurgical technology. It was the first method used to prepare low porosity metals under pressureless sintering. The raw metallic powders remain solid throughout the whole sintering process. The sintered porous metal or metal foam exhibits the typical isolated open morphology because the spherical particles are connected by sinter necks.

In order to obtain materials with higher porosity, more advanced technologies can be used (i.e. using a space holder or hollow spheres, entrapping gas in a powder compact or by slurry coating of polyurethane foams).

A. Conventional powder metallurgy sintering of metal powder

In this case the inner porosity of the resulting compacts results from the “voids” left behind after the powder sintering process of the low-pressure compacted pellets, and the porosity is attributed to the spherical morphology of the powders. Even though the porosity achieved by this method is relatively low compared with others techniques, the simplicity and low cost of the equipment make it a suitable technique to produce different kinds of metals.

B. Space holder additive based on conventional powder metallurgy

In this case, a space holder (porogen) is added to the powder mixture to obtain materials with higher porosity and homogenous pore size. The porous metals or metal foams are produced by mixing the raw powders with the space holder additive which, in turn, sublimates during a thermal treatment process or dissolves leaving numerous pores beneath. Sometimes, in order to further densify the porous metal to obtain higher strength, a second sintering process can be applied. An schematic diagram of the process is shown in Figure 1.6 [122]. The morphology, as well as pore size, depend on the space holder particle size and morphology. The porosity percentage can be tailored by varying the amount of space holder. Water-soluble salts, polymer granules, ceramic or polymer hollow spheres, or even metal powders, can be used as space holders. To eliminate the space holder from the compact, two different strategies can be pursued. In the first one, the space holder (e.g. carbamide granules, Mg grains, etc.) can either thermally decompose, evaporate or sublimate during the sintering process [123]. In this case, the space holder material needs to have good mechanical strength to maintain its structure after compaction. In the second one, the space holder can be dissolved in a solvent (normally water) which does not chemically react with the metal matrix. This approach is used when the melting temperature of the space holder is higher than the sintering temperature of the metal matrix. For instance, Kelhar et al. used $NaAlO_2$, which has a melting temperature of 1800 °C, as space holder to successfully prepare Ni-Mn-Ga metal foams [124].

C. Slurry foaming techniques

This technique involves a slurry produced by mixing metal powders, a polymer and a solvent (water or alcohol). Several approaches can be followed to obtain the slurry. For instance, the slurry can be mechanically agitated until it becomes viscous and starts to expand as a result of the gas bubbles originated because of the foaming agent or chemical reaction. After a while, the fragile and porous structure is sintered under inert or reducing atmospheres to gain structural stability and strength. Angel et al. [125] used Slip-Reaction-Foam-Sintering method to prepare metal-phosphates foams which can withstand a compression strength up to 600 °C. The resulting foams can be used in cooling structures or substrates for catalytic reactions at high temperature. However, this method has also some limitations, such as the unstability of the slurry or the relatively low mechanical strength.

Another approach to produce foams from slurries of metal powders is to prepare highly porous open cell foams using reticulated polyurethane foams. In the last few years, this method has been a subject of intense research. Firstly, the reticulated polyurethane sponge is coated by slurry infiltration. To prevent the pores blockage, the excess of slurry can be removed by squeezing the foam. Secondly, the reticulated polyurethane sponge is removed by thermal decomposition and then the debinded metal is sintered to achieve mechanical strength. Steels foams [126-129] and Cu-based and Ti-based foams have been produced following this approach for permanent biomedical implant applications [130]. In turn, Fe-based foams are also under study because they are considered as promising degradable implants [131, 132].

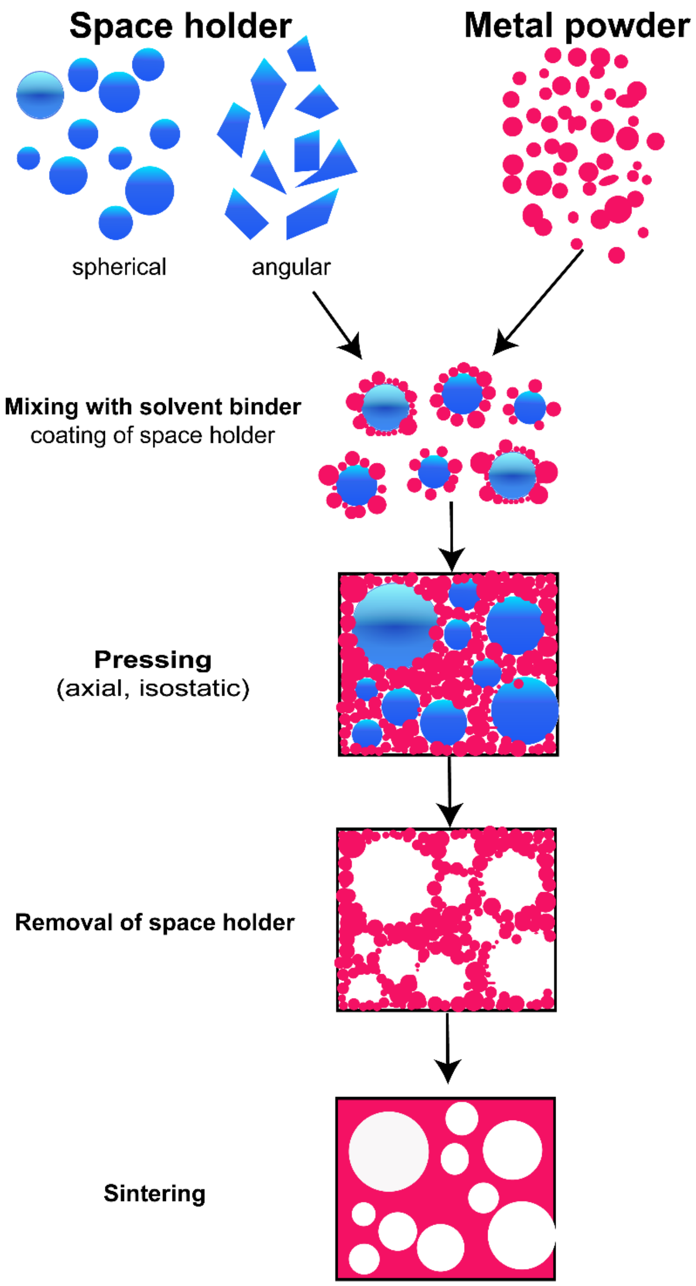

Figure 1.6: Sketch of the process steps followed to produce porous metallic metals using space holder [122].

D. Gas entrapment

Porous metals can be manufactured by a gas expansion process. Firstly, following the same procedure than in conventional PM, the raw metal powders are mixed and compressed in a mold to obtain a compact precursor material. During the compression process, the mold is first evacuated by a vaccum pump; then, argon is entrapped inside the mold. Subsequently, the precursor is heated at high temperature allowing the entrapped argon to form small pores inside the metal. This process is considered to be a solid creep process. Figure 1.7 shows the technological implementation of gas entrapment.

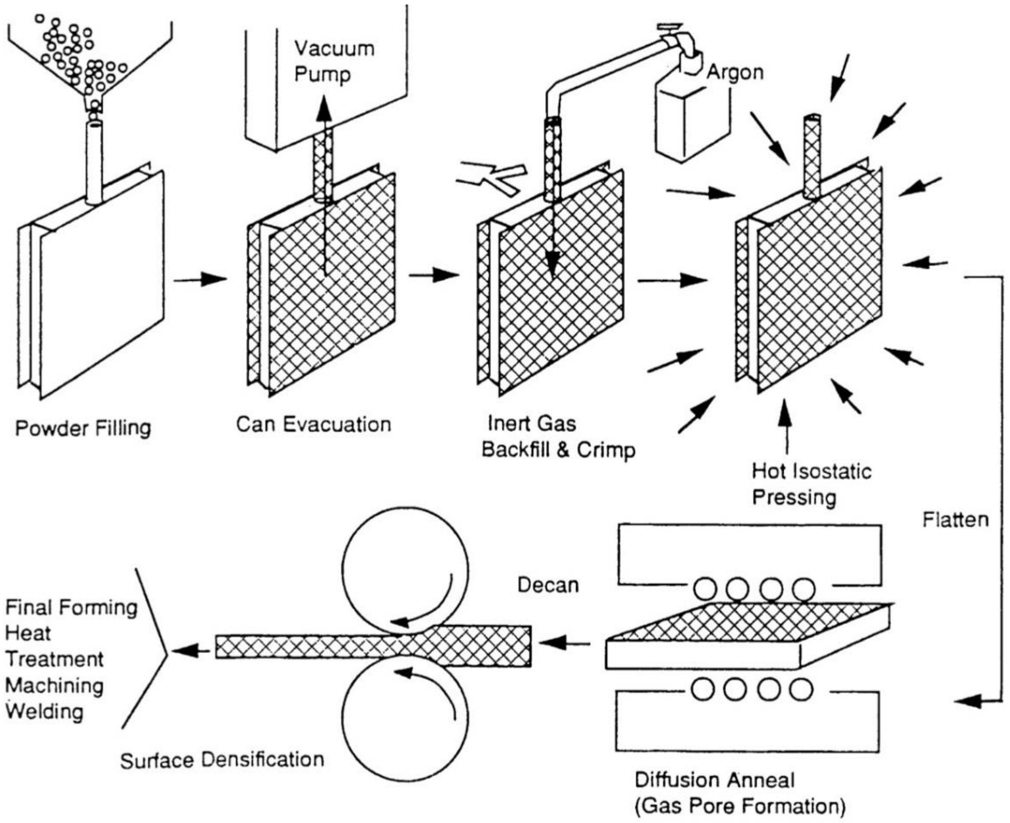

Figure 1.7: Technological implementation of gas entrapment [119].

1.4.2 Cellular metallic materials produced from liquid metal

Molten metals with adjusted viscosities can be foamed by introducing gas bubbles (acting as pore spacers) to the liquid metals. Normally, fine ceramic powders will be added to increase the viscosity of the molten metals, which, in turn, can decrease the buoyancy forces in the high-density melts. Gas injection into the liquid phase or addition of gas-releasing blowing agents are the most common ways to produce foams directly form the liquid.

A. Foaming by gas injection or blowing agent

The porosity produced by direct foaming of the liquid metal comes from the gas bubbles created in the metallic melt. At present, there exist two ways for foaming melts, either by gas injection (air, nitrogen, argon) directly into the liquid metals, or by the in-situ gas formation in the liquid produced by the addition of gas-releasing blowing agents to the molten metal. Figure 1.8 shows the process of foaming melts by gas injection. Large volumes of foam and relatively low densities are the main advantages of this direct foaming method. However, the brittleness of the foam is still a big challenge that needs to be overcome, especially, if further cutting is required. Figure 1.9 shows the process to obtain a foam directly from the melt by the addition of a blowing agent. In this case [134], 1.6% of TiH_2 was added into the powder mixtures (made of Ca and Al) to produce the gas bubbles in the melts at 680 °C.

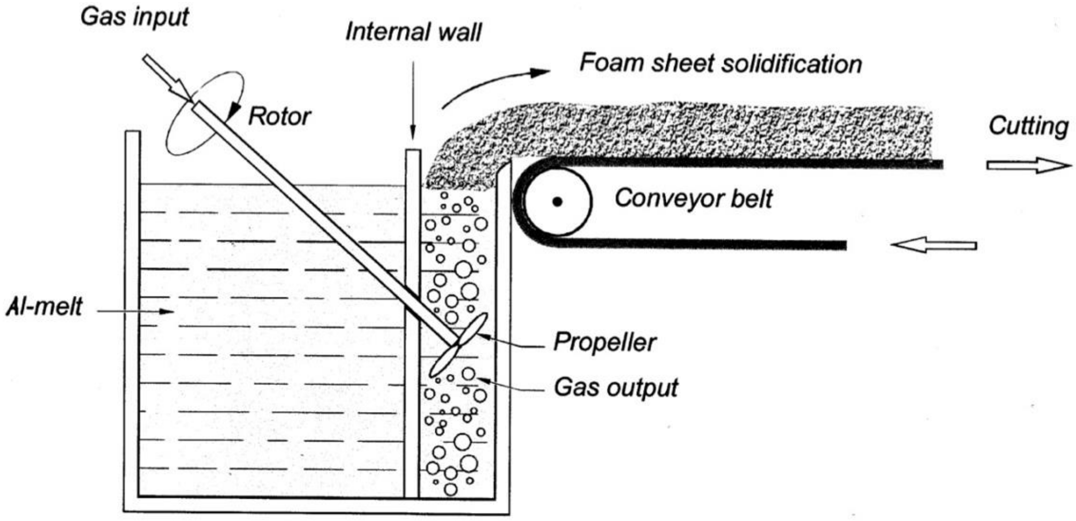

Figure 1.8: Direct foaming of melts by gas injection [133].

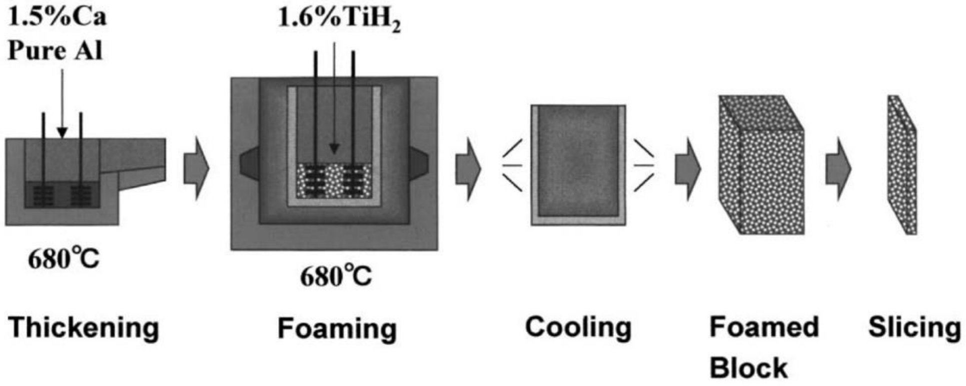

Figure 1.9: Direct foaming of melts by adding blowing agents [134].

B. Solid-gas eutectic solidification (Gasar)

The Gasar method can be used to prepare porous metals based on the fact that some liquid metals can form a eutectic system with H_2 gas. Normally, melting these metals in a H_2 atmosphere under high pressure (up to 50 atm) will result in a homogenous melt with H_2. With a decrease of temperature, heterogeneous two-phase systems (solid + gas) will be formed after the eutectic transition. A segregation reaction between gas and metal will happen at a certain temperature if the composition of the system is close to the eutectic composition range. This can be owed to directional solidification during the process of removal of heat from the melt. Then, the gaseous pores will precipitate and be entrapped in the metal during the process of solidification. The amount of hydrogen, the pressure, and the directional solidification will dictate the pore morphologies [121].

C. Powder compact melting technique

This method basically uses the conventional PM technique to mix the elementary metal powders with a blowing agent in the liquid state to get a homogenous mixture. Dense precursor materials are prepared by compacting the mixture. Then, at the melting temperature of the matrix material, the blowing agent decomposes and the released gas forces the compacted precursor material to expand to achieve the final porous structure. Figure 1.10 shows a sketch of the powder compact melting process.

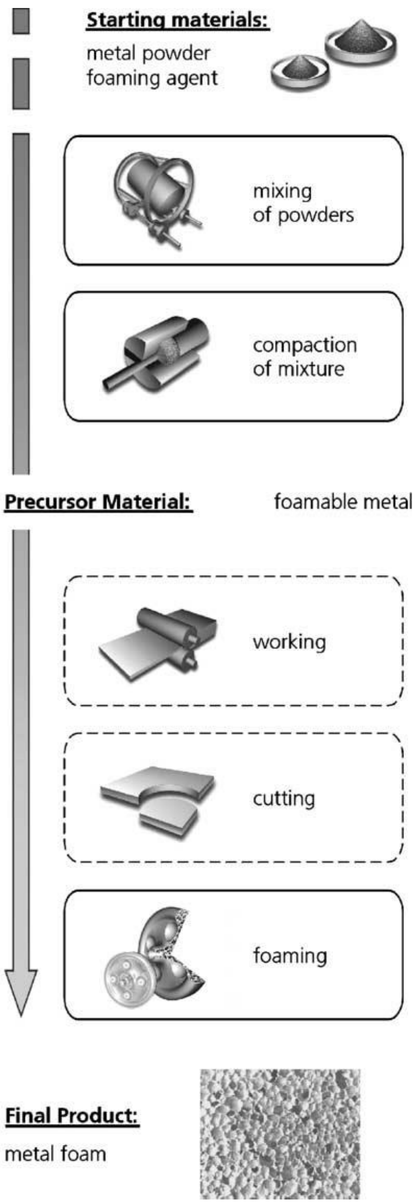

Figure 1.10: Powder compact melting process [133].

1.4.3 Methods to prepare nanoporous metals

As stated in the previous chapters, numerous approaches have been followed to prepare macrocellular foams; however, a lower number of fabrication procedures have been explored to fabricate nanoporous metal materials. Nonetheless, it is worth to notice that nanoporous materials with pore sizes ranging from 1 nm to 100 nm are widely used in different applications because their excellent thermal and electrical conductivity, catalytic activity, and so on. According to the IUPAC definition [135], nanoporous materials can be classified into three groups depending on the pore size (D): microporous ($D < 2$ nm), mesoporous (D = 2-50 nm) and macroporous materials (D > 50 nm). There exist more and more well-established techniques to produce nanoporous materials, no matter whether nanoporous thin films or 3D structured nanoporous metals are considered: dealloying, template-assisted, laser treatment of dense thin films or bulk materials, sol-gel, combustion synthesis, etc.

Some of these methods are explained below:

A. Dealloying

Dealloying is a corrosion process in which the active component of an alloy is selectively dissolved in the appropriate acid/base media. Erlebacher et. al. [136] firstly proposed a continuum model to study the evolution of the porosity and to predict the potential to apply in order to dealloy nanoporous metals (see Figure 1.11). Since then, dealloying is considered as one of most promising methods to manufacture high porosity nanoporous metallic alloys with pore sizes below 100 nm and with bi-continuous pore-ligament structures. During the last few years, many works were focused on developing new methodologies to obtain dealloyed metals and to study their nanoporosity evolution [137]. The working principle of dealloying is to selectively etch away (chemically or electrochemically) the active component of an originally binary or multicomponent system made of components with different equilibrium potentials. During the dissolution process, the less noble elements are removed while the remaining more stable corrosion-resistant material may rearrange to form a 3D interconnected porous framework with open porosity. Parameters like chemical etching conditions, crystal grains scattering, the quantity of the forming phases, and the ratio of metal grains to boundary volume determine the morphology of the materials and the pore structure. Dealloying process is a fast cost-effective method. This is one of the main reasons for the rapidly growing popularity of different dealloyed nanoporous metallic alloys. To date, a growing number of nanoporous metals have been dealloyed to produce nanoporous metals, including nickel [138-140], gold [141-148], copper [149, 150], silver [151], iron [74, 152], platinum [153], or palladium [154].

Until now, two strategies are considered as particularly innovative. The first one consists in using a dealloyed film as template for further deposition. The idea is to deposit a coating on the dealloyed template and then dissolve it away to produce a 3D interconnected metal porous framework (replica). The obtained nanoporous materials are generally thermally stable and show stronger and stiffer mechanical properties than the ones produced by traditional aerogels, mainly due to the narrower pore size distributions. Nanotubular mesoporous Pt [155] or Ti [156] and advanced nanoporous graphene [157, 158] were prepared recently following this method. In addition, not only metals but also organic compounds and oxides can take advantage of this method to yield nanoporous structures. The second method is based on the traditional electrochemical dealloying process which manufactures nanoporous noble—e.g., Au, Pt, and Cu materials by selectively removing metal oxides or metals from multicomponent alloys. Kato et al. proposed an innovative dealloying method called liquid metal dealloying (LMD), which uses molten metals as the dissolution medium to selectively remove one of the alloying components to fabricate nanoporous materials. LMD method can be employed to dealloy precious metals or any kind of metal mixtures, including Cr [159], Fe [74, 159], Si [160], and refractory elements like Nb and Ta [161, 162].

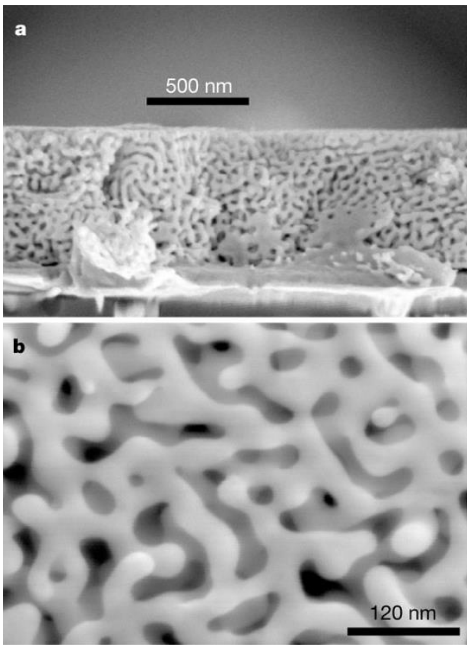

Figure 1.11: SEM image of a dealloyed $Au_{26}Ag_{74}$ thin film a) Cross-section and b) magnified top view [136].

B. Templating method

Templating is considered as the most successful way to produce all sorts of nanoporous materials with a good control over the pore size and pore structure. Various templates including hard templates such as porous anodic aluminum oxide, porous silicon substrate, mesoporous carbon, polymer microspheres, and soft templates such as high density polymers and biopolymers can be used to prepare a series of nanostructured materials such as nanorods, nanowires, nanotubes, and nanobelts. Another advantage of the templating method is that it is sensitive-free to the preparation conditions. The structure, morphology and pore properties are easily tuned by choosing different template materials. Standard processing of nanoporous materials synthesized by employing the templating method can be divided into three steps. First, the template with nano-sized pores is prepared. Secondly, some general synthetic technique such as (electro)chemical deposition method, precipitation, or sol-gel method is used to synthesize the targeted material inside the template channels. Finally, the template is removed by physical or chemical methods like dissolution, sintering, or etching [163].

C. Laser treatment

Direct metal manufacturing additive technologies such as selective laser melting (SLM) have been used to fabricate a wide range of materials, but it was not until few years ago that these methods have been used to produce degradable iron materials. In SLM, metallic powders are mixed with an alloying element and then locally melted, within very small physical zones, by using a laser beam. This procedure usually leads to a rather uniform bulk structure.

Niendorf et al. [164] investigated the selective laser melting technique to fabricate Fe-22Mn-0.6C alloys with silver (Ag) as additional alloying element in different weight percentages. The Fe-22Mn-0.6C alloy exhibits improved biodegradability rate because the well-distributed silver precipitates act as cathodic sites to induce microgalvanic corrosion. The mechanical properties do not show signs of deterioration compared with pure iron. Bandyopadhyay et al. [165] used Laser Engineered Net Shaping to successfully manufacture a series of nanoporous metallic materials or alloys with different degrees of porosity such as Co-Cr-Co, Ti6Al4V and NiTi with promising mechanical and biological properties. Näth et al. [166] used a novel method combining laser etching and phase selective electrolysis to produce nanoporous Ni-based superalloy membranes. This method allows tailoring the pore size and the amount of porosity by tuning the process parameters. In this case, permeable and non-permeable domains were obtained, thus improving the catalytic effectiveness significantly.

1.5 Objectives

In this Thesis, several synthetic procedures such as arc-melting, powder metallurgy, replication method or advanced surface modification techniques have been exploited to produce Fe-based multifunctional materials. Several characterization techniques have been used to shed light onto their physical and physico-chemical properties. In short, the fabrication of novel Fe-based materials to be used in biomedical or environmental applications constitutes the core of this Thesis. In each study, non-conventional material architectures like porous foams or 3D interconnected metal porous frameworks are devised and manufactured to achieve the targeted properties.

The goals of this Thesis can be summarized as follows:

1. To design and fabricate ferromagnetic Fe-10Mn6Si1Pd (wt.%) and shape memory, paramagnetic Fe-30Mn6Si1Pd (wt.%) compact alloys by arc-melting followed by copper mold suction casting. The main purpose is to find suitable quaternary Fe-based bulk alloys with optimized properties to be used in temporary implants. The evolution of microstructure, mechanical and magnetic properties, as well as the assessment of degradation, cytotoxicity and cell proliferation in Hank’s solution as a function of the immersion time are systematically studied.

2. To prepare porous Fe-30Mn6Si1Pd (wt.%) alloys by a simple press and sinter process from ball-milled Fe, Mn, Si and Pd powders blended with 10 wt.%, 20 wt.% and 40 wt.% NaCl. The main purpose is to investigate whether the porous structure can enhance the biodegradation performance

of the material and improve its biomechanical compatibility between an eventual implant and the neighboring bone tissue by lowering its Young's modulus, without compromising the cell viability.

3. To grow calcium phosphate coatings (CaP) (i.e., brushite and hydroxyapatite) at the surface of Fe-10Mn6Si1Pd alloys by pulsed current electrodeposition. The main purpose is to control the crystallographic structure of the coatings and their morphology by adjusting the electrodeposition parameters, aiming at optimizing the adherence of the coatings to the alloys.

4. To prepare open cell foams consisting of Fe and Fe-Mn oxides from metallic Fe and Mn powder precursors by the replication method using porous polyurethane templates. The main goal here is to tailor the magnetic response of the foams from virtually non-magnetic to ferrimagnetic by controllably adjusting the Mn content as well as the N_2 flow rate.

5. To synthesize a fully nanoporous Fe-rich alloy by selective dissolution of melt-spun $Fe_{43.5}Cu_{56.5}$ ribbons. The main objective is to obtain wirelessly-manipulated, magnetic, Fe-based heterogeneous Fenton catalyst with high catalytic activity.

6. To form periodic ripple and nanoripple patterns at the surface of amorphous steel by femtosecond pulse laser irradiation. The main goal is to adjust both the topological damage as well as the composition of the alloy at surface level, resulting in local modifications of some of the physical properties (e.g., magnetic response, mechanical strength, etc.) of these materials at the surface.

References

[1] N.E. Holden, History of the origin of the chemical elements and their discoverers, in processing of 41st IUPAC General Assembly in Brisbane, June 29-July 8, 2001.

[2] A. Domashenkov, A. Plotnikova, I. Movchan, P. Bertrand, N. Peillon, B. Desplanques, S. Saunier, C. Desrayaud, Microstructure and physical properties of a Ni/Fe-based superalloy processed by Selective Laser Melting, Additive Manufacturing 15 (2017) 66-77.

[3] A. Cladera, B. Weber, C. Leinenbach, C. Czaderski, M. Shahverdi, M. Motavalli, Iron-based shape memory alloys for civil engineering structures: An overview, Construction and Building Materials 63 (2014) 281-293.

[4] J. Ding, W.F. Miao, P.G. McCormick, R. Street, High-coercivity ferrite magnets prepared by mechanical alloying, Journal of Alloys and Compounds 281 (1998) 32-36.

[5] M.W. Tibbitt, C.B. Rodell, J.A. Burdick, K.S. Anseth, Progress in material design for biomedical applications, Proceedings of the National Academy of Sciences 112 (2015) 14444-14451.

[6] M. Moravej, D. Mantovani, Biodegradable metals for cardiovascular stent application: interests and new opportunities, International Journal of Molecular Sciences 12 (2011) 4250-4270.

[7] J. Park, R.S. Lakes, Biomaterials: an introduction, Springer Science and Business Media 2007.

[8] T.J. Webster, Nanotechnology enabled in situ sensors for monitoring health, Springer Science and Business Media 2010.

[9] F. Witte, Reprint of: The history of biodegradable magnesium implants: A review, Acta Biomaterialia 23 (2015) S28-S40.

[10] F. Zivic, S. Affatato, M. Trajanovic, M. Schnabelrauch, N. Grujovic, K. L. Choy, Biomaterials in clinical practice-advances in clinical research and medical devices, Chapter 9, Springer International Publishing, 2017.

[11] Y.F. Zheng, X.N. Gu, F. Witte, Biodegradable metals, Materials Science and Engineering: R: Reports 77 (2014) 1-34.

[12] H.F. Li, Y.F. Zheng, L. Qin, Progress of biodegradable metals, Progress in Natural Science: Materials International 24 (2014) 414-422.

[13] L.P. Xu, G.N. Yu, E. Zhang, F. Pan, K. Yang, In *vivo* corrosion behavior of Mg-Mn-Zn alloy for bone implant application, Journal of Biomedical Materials Research Part A 83 (2007) 703-711.

[14] Z.J. Li, X.N. Gu, S.Q. Lou, Y.F. Zheng, The development of binary Mg-Ca alloys for use as biodegradable materials within bone, Biomaterials 29 (2008) 1329-1344.

[15] F. Witte, N. Hort, C. Vogt, S. Cohen, K.U. Kainer, R. Willumeit, F. Feyerabend, Degradable biomaterials based on magnesium corrosion, Current Opinion in Solid State and Materials Science 12 (2008) 63-72.

[16] A.C. Hanzi, P. Gunde, M. Schinhammer, P.J. Uggowitzer, On the biodegradation performance of an Mg-Y-RE alloy with various surface conditions in simulated body fluid, Acta Biomaterialia 5 (2009) 162-171.

[17] H.F. Li, X.H. Xie, K. Zhao, Y.B. Wang, Y.F. Zheng, W.H. Wang, L. Qin, In *vitro* and in *vivo* studies on biodegradable CaMgZnSrYb high-entropy bulk metallic glass, Acta Biomaterialia 9 (2013) 8561-8573.

[18] D.T. Chou, D. Wells, D. Hong, B. Lee, H. Kuhn, P.N. Kumta, Novel processing of iron-manganese alloy-based biomaterials by inkjet 3-D printing, Acta Biomaterialia 9 (2013) 8593-8603.

[19] B. Liu, Y.F. Zheng, Effects of alloying elements (Mn, Co, Al, W, Sn, B, C and S) on biodegradability and in *vitro* biocompatibility of pure iron, Acta Biomaterialia 7 (2011) 1407-1420.

[20] M. Moravej, F. Prima, M. Fiset, D. Mantovani, Electroformed iron as new biomaterial for degradable stents: Development process and structure-properties relationship, Acta Biomaterialia 6 (2010) 1726-1735.

[21] M. Moravej, A. Purnama, M. Fiset, J. Couet, D. Mantovani, Electroformed pure iron as a new biomaterial for degradable stents: In *vitro* degradation and preliminary cell viability studies, Acta Biomaterialia 6 (2010) 1843-1851.

[22] M. Schinhammer, A.C. Hanzi, J.F. Löffler, P.J. Uggowitzer, Design strategy for biodegradable Fe-based alloys for medical applications, Acta Biomaterialia 6 (2010) 1705-1713.

[23] J. Cheng, T. Huang, Y.F. Zheng, Microstructure, mechanical property, biodegradation behavior, and biocompatibility of biodegradable Fe-Fe_2O_3 composites, Journal of Biomedical Materials Research Part A 102 (2014) 2277-2287.

[24] J. Cheng, Y.F. Zheng, In *vitro* study on newly designed biodegradable Fe-X composites (X = W, CNT) prepared by spark plasma sintering, Journal of Biomedical Materials Research Part B 101 (2013) 485-497.

[25] B. Liu, Y.F. Zheng, L.Q. Ruan, In *vitro* investigation of Fe30Mn6Si shape memory alloy as potential biodegradable metallic material, Materials Letters 65 (2011) 540-543.

[26] T. Huang, J. Cheng, Y.F. Zheng, In *vitro* degradation and biocompatibility of Fe-Pd and Fe-Pt composites fabricated by spark plasma sintering, Materials Science and Engineering: C 35 (2014) 43-53.

[27] M. Schinhammer, I. Gerber, A.C. Hanzi, P.J. Uggowitzer, On the cytocompatibility of biodegradable Fe-based alloys, Materials Science and Engineering: C 33 (2013) 782-789.

[28] A.H. Yusop, N.M. Daud, H. Nur, M.R.A. Kadir, H. Hermawan, Controlling the degradation kinetics of porous iron by poly(lactic-co-glycolic acid) infiltration for use as temporary medical implants, Scientific Reports 5 (2015) 11194.

[29] B. Wegener, B. Sievers, S. Utzschneider, P. Muller, V. Jansson, S. Rossler, B. Nies, G. Stephani, B. Kieback, P. Quadbeck, Microstructure, cytotoxicity and corrosion of powder-metallurgical iron alloys for biodegradable bone replacement materials, Materials Science and Engineering: B 176 (2011) 1789-1796.

[30] M. Schinhammer, P. Steiger, F. Moszner, J.F. Löffler, P.J. Uggowitzer, Degradation performance of biodegradable FeMnC(Pd) alloys, Materials Science and Engineering: C 33 (2013) 1882-1893.

[31] M. Schinhammer, C.M. Pecnik, F. Rechberger, A.C. Hanzi, J.F. Löffler, P.J. Uggowitzer, Recrystallization behavior, microstructure evolution and mechanical properties of biodegradable Fe-Mn-C(-Pd) TWIP alloys, Acta Materialia 60 (2012) 2746-2756.

[32] C.S. Obayi, R. Tolouei, C. Paternoster, S. Turgeon, B.A. Okorie, D.O. Obikwelu, G. Cassar, J. Buhagiar, D. Mantovani, Influence of cross-rolling on the micro-texture and biodegradation of pure iron as biodegradable material for medical implants, Acta Biomaterialia 17 (2015) 68-77.

[33] F. Moszner, A.S. Sologubenko, M. Schinhammer, C. Lerchbacher, A.C. Hanzi, H. Leitner, P.J. Uggowitzer, J.F. Löffler, Precipitation hardening of biodegradable Fe-Mn-Pd alloys, Acta Materialia 59 (2011) 981-991.

[34] T. Kraus, F. Moszner, S. Fischerauer, M. Fiedler, E. Martinelli, J. Eichler, F. Witte, E. Willbold, M. Schinhammer, M. Meischel, P.J. Uggowitzer, J.F. Löffler, A. Weinberg, Biodegradable Fe-based alloys for use in osteosynthesis: outcome of an in *vivo* study after 52 weeks, Acta Biomaterialia 10 (2014) 3346-3353.

[35] D.H. Hong, D.T. Chou, O.I. Velikokhatnyi, A. Roy, B. Lee, I. Swink, I. Issaev, H.A. Kuhn, P.N. Kumta, Binder-jetting 3D printing and alloy development of new biodegradable Fe-Mn-Ca/Mg alloys, Acta Biomaterialia 45 (2016) 375-386.

[36] H. Hermawan, A. Purnama, D. Dubé, J. Couet, D. Mantovani, Fe-Mn alloys for metallic biodegradable stents: degradation and cell viability studies, Acta Biomaterialia 6 (2010) 1852-1860.

[37] Y.P. Feng, A. Blanquer, J. Fornell, H.Y. Zhang, P. Solsona, M.D. Baro, S. Surinach, E. Ibanez, E. García-Lecina, X.Q. Wei, R. Li, L. Barrios, E. Pellicer, C. Nogues, J. Sort, Novel Fe-Mn-Si-Pd alloys: insights into mechanical, magnetic, corrosion resistance and biocompatibility performances, Journal of Materials Chemistry B 4 (2016) 6402-6412.

[38] J. Cheng, B. Liu, Y.H. Wu, Y.F. Zheng, Comparative in *vitro* study on pure metals (Fe, Mn, Mg, Zn and W) as biodegradable metals, Journal of Materials Science and Technology 29 (2013) 619-627.

[39] J. Capek, D. Vojtech, A. Oborna, Microstructural and mechanical properties of biodegradable iron foam prepared by powder metallurgy, Materials and Design 83 (2015) 468-482.

[40] N.B. Sing, A. Mostavan, E. Hamzah, D. Mantovani, H. Hermawan, Degradation behavior of biodegradable Fe35Mn alloy stents, Journal of Biomedical Materials Research Part B 103 (2015) 572-577.

[41] H. Hermawan, D. Mantovani, Process of prototyping coronary stents from biodegradable Fe-Mn alloys, Acta Biomaterialia 9 (2013) 8585-8592.

[42] H. Hermawan, D. Dubé, D. Mantovani, Degradable metallic biomaterials: design and development of Fe-Mn alloys for stents, Journal of Biomedical Materials Research Part A 93 (2010) 1-11.

[43] N.S. Fagali, C.A. Grillo, S. Puntarulo, M.A. Fernandez Lorenzo de Mele, Cytotoxicity of corrosion products of degradable Fe-based stents: relevance of pH and insoluble products, Colloids and Surfaces B: Biointerfaces 128 (2015) 480-488.

[44] M. Dehestani, E. Adolfsson, L.A. Stanciu, Mechanical properties and corrosion behavior of powder metallurgy iron-hydroxyapatite composites for biodegradable implant applications, Materials and Design 109 (2016) 556-569.

[45] E. Mouzou, C. Paternoster, R. Tolouei, A. Purnama, P. Chevallier, D. Dubé, F. Prima, D. Mantovani, In *vitro* degradation behavior of Fe-20Mn-1.2C alloy in three different pseudo-physiological solutions, Materials Science and Engineering: C 61 (2016) 564-573.

[46] N.M. Daud, N.B. Sing, A.H. Yusop, F.A.A. Majid, H. Hermawan, Degradation and in *vitro* cell–material interaction studies on hydroxyapatite-coated biodegradable porous iron for hard tissue scaffolds, Journal of Orthopaedic Translation 2 (2014) 177-184.

[47] H. Hermawan, H. Alamdari, D. Mantovani, D. Dubé, Iron-manganese: new class of metallic degradable biomaterials prepared by powder metallurgy, Powder Metallurgy 51 (2008) 38-45.

[48] W. Jiao, K. Zhao, X.K. Xi, D.Q. Zhao, M.X. Pan, W.H. Wang, Zinc-based bulk metallic glasses, Journal of Non-Crystalline Solids 356 (2010) 1867-1870.

[49] P.K. Bowen, J. Drelich, J. Goldman, Zinc exhibits ideal physiological corrosion behavior for bioabsorbable stents, Advanced Materials 25 (2013) 2577-2582.

[50] Y.B. Wang, X.H. Xie, H.F. Li, X.L. Wang, M.Z. Zhao, E.W. Zhang, Y.J. Bai, Y. F. Zheng, L. Qin, Biodegradable CaMgZn bulk metallic glass for potential skeletal application, Acta Biomaterialia 7 (2011) 3196-3208.

[51] K. Zhao, J.F. Li, D.Q. Zhao, M.X. Pan, W.H. Wang, Degradable Sr-based bulk metallic glasses, Scripta Materialia 61 (2009) 1091-1094.

[52] K. Zhao, W. Jiao, J. Ma, X.Q. Gao, W.H. Wang, Formation and properties of strontium-based bulk metallic glasses with ultralow glass transition temperature, Journal of Materials Research 27 (2012) 2593-2600.

[53] M. Peuster, P. Wohlsein, M. Brügmann, M. Ehlerding, K. Seidler, C. Fink, H. Brauer, A. Fischer, G. Hausdorf, A novel approach to temporary stenting: degradable cardiovascular stents produced from corrodible metal—results 6–18 months after implantation into New Zealand white rabbits, Heart 86 (2001) 563-569.

[54] M. Peuster, C. Hesse, T. Schloo, C. Fink, P. Beerbaum, C.V. Schnakenburg, Long-term biocompatibility of a corrodible peripheral iron stent in the porcine descending aorta, Biomaterials 27 (2006) 4955-4962.

[55] F. Moszner, Fe–Mn–Pd maraging steels for biodegradable implant applications, Doctoral Dissertation, Eidgenössische Technische Hochschule ETH Zürich, 2014.

[56] F. Moszner, E. Povoden-Karadeniz, S. Pogatscher, P.J. Uggowitzer, Y. Estrin, S.S.A. Gerstl, E. Kozeschnik, J.F. Löffler, Reverse α′→ γ transformation mechanisms of martensitic Fe–Mn and age-hardenable Fe–Mn–Pd alloys upon fast and slow continuous heating, Acta Materialia 72 (2014) 99-109.

[57] F. Moszner, S.S.A. Gerstl, P.J. Uggowitzer, J.F. Löffler, Structural and chemical characterization of the hardening phase in biodegradable Fe-Mn-Pd maraging steels, Journal of Materials Research 29 (2014) 1069-1076.

[58] F. Moszner, S.S.A. Gerstl, P.J. Uggowitzer, J.F. Löffler, Atomic-scale characterization of prior austenite grain boundaries in Fe-Mn-based maraging steel using site-specific atom probe tomography, Acta Materialia 73 (2014) 215-226.

[59] H. Hermawan, D. Dubé, D. Mantovani, Development of Degradable Fe-35Mn Alloy for Biomedical Application, Advanced Materials Research 15-17 (2007) 107-112.

[60] W.L. Xu, X. Lu, L.L. Tan, K. Yang, Study on properties of a novel biodegradable Fe–30Mn–1C alloy, Acta Metallurgica Sinica 47 (2011) 1342-1347.

[61] Q. Zhang, P. Cao, Degradable porous Fe-35wt.%Mn produced via powder sintering from NH_4HCO_3 porogen, Materials Chemistry and Physics 163 (2015) 394-401.

[62] X.N. Gu, Y.F. Zheng, S.P. Zhong, T.F. Xi, J.Q. Wang, W.H. Wang, Corrosion of, and cellular responses to Mg-Zn-Ca bulk metallic glasses, Biomaterials 31 (2010) 1093-1103.

[63] L.J. Gibson, M.F. Ashby, Cellular solids: structure and properties, Cambridge University Press,1999.

[64] E. Aghion, T. Yered, Y. Perez, Y. Gueta, The Prospects of Carrying and Releasing Drugs Via Biodegradable Magnesium Foam, Advanced Engineering Materials 12 (2010) B374-B379.

[65] X. Li, C. Chu, Y. Wei, C. Qi, J. Bai, C. Guo, F. Xue, P. Lin, P.K. Chu, In *vitro* degradation kinetics of pure PLA and Mg/PLA composite: Effects of immersion temperature and compression stress, Acta Biomaterialia 48 (2017) 468-478.

[66] J. Cheng, T. Huang, Y.F. Zheng, Relatively uniform and accelerated degradation of pure iron coated with micro-patterned Au disc arrays, Materials Science and Engineering: C 48 (2015) 679-687.

[67] N. Cimpoesu, L.C. Trinca, G. Dascalu, S. Stanciu, S.O. Gurlui, D. Mareci, Electrochemical characterization of a new biodegradable FeMnSi Alloy coated with hydroxyapatite-zirconia by PLD technique, Journal of Chemistry 2016 (2016) 9520972.

[68] M.H.P.D. Silva, G.A. Soares, C.N. Elias, I.R. Gibson, S.M. Best, Bioactivity assessment of hydroxyapatite coatings produced by alkali conversion of monetite, Key Engineering Materials 192-195 (2001) 59-62.

[69] R. Rohanizadeh, R.Z. LeGeros, M. Harsono, A. Bendavid, Adherent apatite coating on titanium substrate using chemical deposition, Journal of Biomedical Materials Research Part A 72 (2005) 428-438.

[70] A.S. Adeleye, J.R. Conway, K. Garner, Y.X. Huang, Y.M. Su, A.A. Keller, Engineered nanomaterials for water treatment and remediation: Costs, benefits, and applicability, Chemical Engineering Journal 286 (2016) 640-662.

[71] J.C. Ng, J. Wang, A. Shraim, A global health problem caused by arsenic from natural sources, Chemosphere 52 (2003) 1353-1359.

[72] D. Grey, D. Garrick, D. Blackmore, J. Kelman, M. Muller, C. Sadoff, Water security in one blue planet: twenty-first century policy challenges for science, Philosophical Transactions of the Royal Society A 371 (2013) 20120406.

[73] R.P. Schwarzenbach, B.I. Escher, K. Fenner, T.B. Hofstetter, C.A. Johnson, U. von Gunten, B. Wehrli, The challenge of micropollutants in aquatic systems, Science 313 (2006) 1072-1077.

[74] H.Y. Zhang, Y.P. Feng, Y.Y. Cheng, M.D. Baro, A. Altube, E. García-Lecina, F. Alcaide, E. Pellicer, T. Zhang, J. Sort, Nanoporous Fe-based alloy prepared by selective dissolution: an effective fenton catalyst for water remediation, ACS Omega 2 (2017) 653-662.

[75] X.L. Qu, J. Brame, Q.L. Li, P.J.J. Alvarez, Nanotechnology for a safe and sustainable water supply: enabling integrated water treatment and reuse, Accounts of Chemical Research 46(3) (2013) 834-843.

[76] E.Ç. Çatalkaya, U. Bali, F. Şengül, Photochemical degradation and mineralization of 4-chlorophenol, Environmental Science and Pollution Research 10 (2003) 113-120.

[77] U. Bali, E.Ç. Çatalkaya, F. Şengül, Photochemical degradation and mineralization of phenol: a comparative study, Journal of Environmental Science and Health Part A 38 (2003) 2259-2275.

[78] A. Georgi, F.D. Kopinke, Interaction of adsorption and catalytic reactions in water decontamination processes Part I. Oxidation of organic contaminants with hydrogen peroxide catalyzed by activated carbon, Applied Catalysis B 58 (2005) 9-18.

[79] Y. Yoshida, S. Ogata, S. Nakamatsu, T. Shimamune, K. Kikawa, H. Inoue, C. Iwakura, Decoloration of azo dye using atomic hydrogen permeating through a Pt-modified palladized Pd sheet electrode, Electrochimica Acta 45 (1999) 409-414.

[80] K. Dutta, S. Mukhopadhyay, S. Bhattacharjee, B. Chaudhuri, Chemical oxidation of methylene blue using a Fenton-like reaction, Journal of Hazardous Materials 84 (2001) 57-71.

[81] K. Zare, F. Najafi, H. Sadegh, R.S. Ghoshekandi, Studies of *ab initio* and Monte Carlo simulation on interaction of fluorouracil anticancer drug with carbon nanotube, Journal of Nanostructure in Chemistry 3 (2013) 71.

[82] M. Ozmen, K. Can, G. Arslan, A. Tor, Y. Cengeloglu, M. Ersoz, Adsorption of Cu(II) from aqueous solution by using modified Fe_3O_4 magnetic nanoparticles, Desalination 254 (2010) 162-169.

[83] T. Luo, J.L. Cui, S. Hu, Y.Y. Huang, C.Y. Jing, Arsenic removal and recovery from copper smelting wastewater using TiO_2, Environmental Science and Technology 44 (2010) 9094-9098.

[84] C.L. Gao, W.L. Zhang, H.B. Li, L.M. Lang, Z. Xu, Controllable fabrication of mesoporous MgO with various morphologies and their absorption performance for toxic pollutants in water, Crystal Growth and Design 8 (2008) 3785-3790.

[85] S. Singh, K. Barick, D. Bahadur, Fe_3O_4 embedded ZnO nanocomposites for the removal of toxic metal ions, organic dyes and bacterial pathogens, Journal of Materials Chemistry A 1 (2013) 3325-3333.

[86] K.E. Engates, H.J. Shipley, Adsorption of Pb, Cd, Cu, Zn, and Ni to titanium dioxide nanoparticles: effect of particle size, solid concentration, and exhaustion, Environmental Science and Pollution Research 18 (2011) 386-395.

[87] Y.H. Li, J. Ding, Z.K. Luan, Z.C. Di, Y.F. Zhu, C.L. Xu, D.H. Wu, B.Q. Wei, Competitive adsorption of Pb^{2+}, Cu^{2+} and Cd^{2+} ions from aqueous solutions by multiwalled carbon nanotubes, Carbon 41 (2003) 2787-2792.

[88] Y.H. Li, S.G. Wang, Z.K. Luan, J. Ding, C.L. Xu, D.H. Wu, Adsorption of cadmium(II) from aqueous solution by surface oxidized carbon nanotubes, Carbon 41 (2003) 1057-1062.

[89] G. Lefèvre, J. Kneppers, M. Fédoroff, Sorption of uranyl ions on titanium oxide studied by ATR-IR spectroscopy, Journal of Colloid and Interface Science 327 (2008) 15-20.

[90] C.T. Yavuz, J. Mayo, W.Y. William, A. Prakash, J.C. Falkner, S. Yean, L. Cong, H.J. Shipley, A. Kan, M. Tomson, Low-field magnetic separation of monodisperse Fe_3O_4 nanocrystals, Science 314 (2006) 964-967.

[91] R.J. Bhargavi, U. Maheshwari, S. Gupta, Synthesis and use of alumina nanoparticles as an adsorbent for the removal of Zn(II) and CBG dye from wastewater, International Journal of Industrial Chemistry 6 (2015) 31-41.

[92] V.K. Gupta, A. Nayak, S. Agarwal, I. Tyagi, Potential of activated carbon from waste rubber tire for the adsorption of phenolics: effect of pre-treatment conditions, Journal of Colloid and Interface Science 417 (2014) 420-430.

[93] J. Feng, D.D. Zhang, Y.F. Liu, Y. Bai, Q.D. Chen, S.Y. Liu, H.B. Sun, Magnetic nanofilm of Fe_3O_4 for highly efficient organic light-emitting devices, Journal of Physical Chemistry C 114 (2010) 6718-6721.

[94] Z.Q. Wang, D.Y. Wu, G.H. Wu, N.N. Yang, A.G. Wu, Modifying Fe_3O_4 microspheres with rhodamine hydrazide for selective detection and removal of Hg^{2+} ion in water, Journal of Hazardous Materials 244-245 (2013) 621-627.

[95] H. Wang, X.Z. Yuan, Y. Wu, G.M. Zeng, X.H. Chen, L.J. Leng, Z.B. Wu, L.B. Jiang, H. Li, Facile synthesis of amino-functionalized titanium metal-organic frameworks and their superior visible-light photocatalytic activity for Cr(VI) reduction, Journal of Hazardous Materials 286 (2015) 187-194.

[96] S. Yean, L. Cong, C.T. Yavuz, J.T. Mayo, W.W. Yu, A.T. Kan, V.L. Colvin, M.B. Tomson, Effect of magnetite particle size on adsorption and desorption of arsenite and arsenate, Journal of Materials Research 20 (2005) 3255-3264.

[97] F. Ge, M.M. Li, H. Ye, B.X. Zhao, Effective removal of heavy metal ions Cd^{2+}, Zn^{2+}, Pb^{2+}, Cu^{2+} from aqueous solution by polymer-modified magnetic nanoparticles, Journal of Hazardous Materials 211-212 (2012) 366-372.

[98] C. Zhang, J.H. Sui, J. Li, Y.L. Tang, W. Cai, Efficient removal of heavy metal ions by thiol-functionalized superparamagnetic carbon nanotubes, Chemical Engineering Journal 210 (2012) 45-52.

[99] B.S. Tawabini, Removal of methyl tertiary butyl ether (MTBE) from contaminated water using UV-assisted nano composite materials, Desalination and Water Treatment 55 (2015) 549-554.

[100] M. Kurian, D.S. Nair, Heterogeneous Fenton behavior of nano nickel zinc ferrite catalysts in the degradation of 4-chlorophenol from water under neutral conditions, Journal of Water Process Engineering 8 (2015) e37-e49.

[101] A.K. Dutta, S.K. Maji, B. Adhikary, γ-Fe_2O_3 nanoparticles: an easily recoverable effective photo-catalyst for the degradation of rose bengal and methylene blue dyes in the waste-water treatment plant, Materials Research Bulletin 49 (2014) 28-34.

[102] S. Chaturvedi, P.N. Dave, N.K. Shah, Applications of nano-catalyst in new era, Journal of Saudi Chemical Society 16 (2012) 307-325.

[103] H.Y. Ma, H.T. Wang, C.Z. Na, Microwave-assisted optimization of platinum-nickel nanoalloys for catalytic water treatment, Applied Catalysis B 163 (2015) 198-204.

[104] A. Ali, H. Zafar, M. Zia, I. ul Haq, A.R. Phull, J.S. Ali, A. Hussain, Synthesis, characterization, applications, and challenges of iron oxide nanoparticles, Nanotechnology, Science and Applications 9 (2016) 49-67.

[105] P.R. Gogate, A.B. Pandit, A review of imperative technologies for wastewater treatment I: oxidation technologies at ambient conditions, Advances in Environmental Research 8 (2004) 501-551.

[106] I. Casero, D. Sicilia, S. Rubio, D. Pérez-Bendito, Chemical degradation of aromatic amines by Fenton's reagent, Water Research 31 (1997) 1985-1995.

[107] W.G. Kuo, Decolorizing dye wastewater with Fenton's reagent, Water Research 26 (1992) 881-886.

[108] S. Nam, V. Renganathan, P.G. Tratnyek, Substituent effects on azo dye oxidation by the Fe^{III}–EDTA–H_2O_2 system, Chemosphere 45 (2001) 59-65.

[109] K. Barbusiński, The modified Fenton process for decolorization of dye wastewater, Polish Journal of Environmental Studies 14 (2005) 281-285.

[110] E. Brillas, I. Sirés, M.A. Oturan, Electro-Fenton process and related electrochemical technologies based on Fenton’s reaction chemistry, Chemical Reviews 109 (2009) 6570-6631.

[111] S.M. Arnold, W.J. Hickey, R.F. Harris, Degradation of Atrazine by Fenton's Reagent: Condition Optimization and Product Quantification, Environmental Science and Technology 29 (1995) 2083-2089.

[112] J.A. Zazo, J.A. Casas, A.F. Mohedano, J.J. Rodriguez, Catalytic wet peroxide oxidation of phenol with a Fe/active carbon catalyst, Applied Catalysis B 65 (2006) 261-268.

[113] V.K. Sharma, Ferrate(VI) and ferrate(V) oxidation of organic compounds: kinetics and mechanism, Coordination Chemistry Reviews 257 (2013) 495-510.

[114] M. Hartmann, S. Kullmann, H. Keller, Wastewater treatment with heterogeneous Fenton-type catalysts based on porous materials, Journal of Materials Chemistry 20 (2010) 9002-9017.

[115] H.Y. Xu, S.Y. Qi, Y. Li, Y. Zhao, J.W. Li, Heterogeneous Fenton-like discoloration of Rhodamine B using natural schorl as catalyst: optimization by response surface methodology, Environmental Science and Pollution Research 20 (2013) 5764-5772.

[116] S. Karthikeyan, A. Titus, A. Gnanamani, A.B. Mandal, G. Sekaran, Treatment of textile wastewater by homogeneous and heterogeneous Fenton oxidation processes, Desalination 281 (2011) 438-445.

[117] M.A. Fontecha-Cámara, M.A. Álvarez-Merino, F. Carrasco-Marín, M.V. López-Ramón, C. Moreno-Castilla, Heterogeneous and homogeneous Fenton processes using activated carbon for the removal of the herbicide amitrole from water, Applied Catalysis B 101 (2011) 425-430.

[118] G. Calleja, J.A. Melero, F. Martinez, R. Molina, Activity and resistance of iron-containing amorphous, zeolitic and mesostructured materials for wet peroxide oxidation of phenol, Water Research 39 (2005) 1741-1750.

[119] K. Rusevova, F.D. Kopinke, A. Georgi, Nano-sized magnetic iron oxides as catalysts for heterogeneous Fenton-like reactions-Influence of Fe(II)/Fe(III) ratio on catalytic performance, Journal of Hazardous Materials 241-242 (2012) 433-440.

[120] A. Babuponnusami, K. Muthukumar, Removal of phenol by heterogenous photo electro Fenton-like process using nano-zero valent iron, Separation and Purification Technology 98 (2012) 130-135.

[121] J. Banhart, Manufacture, characterisation and application of cellular metals and metal foams, Progress in Materials Science 46 (2001) 559-632.

[122] M. Bram, C. Stiller, H.P. Buchkremer, D. Stöver, H. Baur, High-porosity Titanium, stainless steel, and superalloy parts, Advanced Engineering Materials 2 (2000) 196-199.

[123] A. Kennedy, Porous metals and metal foams made from powders, in Power Metallurgy, INTECH Open Access Publisher, 2012.

[124] I. Naglič, K.Ž. Rozman, P. McGuiness, L. Kelhar, S. Kobe, B. Markoli, Production of Ni-Mn-Ga foam, RMZ–M&G 60 (2013) 191-196.

[125] S. Angel, W. Bleck, D. Hajas, Y. Jiang, J. Schneider, Inconel 625 foams produced by the SlipReactionFoam-Sintering (SRFS)-process for high temperature applications, in processing of the Fifth International Conference on Porous Metals and Metallic Foams, Montreal Canada, September 5-7, 2007.

[126] Y. Conde, J.F. Despois, R. Goodall, A. Marmottant, L. Salvo, C. San Marchi, A. Mortensen, Replication processing of highly porous materials, Advanced Engineering Materials 8 (2006) 795-803.

[127] P Quadbeck, G Stephani, K Kümmel, J. Adler, G. Standke, Synthesis and properties of open-celled metal foams, processing in Materials Science Forum 534-536 (2007) 1005-1008.

[128] G. Stephani, O. Andersen, P. Quadbeck, B. Kieback, Cellular metals for functional applications – an overview, in processing of PM2010 World Congress – Foams and Porous Materials, Dresden, Germany, 2010.

[129] P. Quadbeck, R. Hauser, K. Kümmel, G. Standke, G. Stephani, B. Nies, S. Rößler, B. Wegener, Iron based cellular metals for degradable synthetic bone replacement, in processing of PM2010 World Congress – PM Biomaterials, Dresden, Germany, 2010.

[130] H. Tiainen, S.P. Lyngstadaas, J.E. Ellingsen, H.J. Haugen, Ultra-porous titanium oxide scaffold with high compressive strength, Journal of Materials Science: Materials in Medicine 21 (2010) 2783-2792.

[131] A.H. Yusop, A.A. Bakir, N.A. Shaharom, M.R. Abdul Kadir, H. Hermawan, Porous biodegradable metals for hard tissue scaffolds: a review, International Journal of Biomaterials 2012 (2012) 641430.

[132] A. Oriňák, R. Oriňáková, Z.O. Králová, A.M. Turoňová, M. Kupková, M. Hrubovčáková, J. Radoňák, R. Džunda, Sintered metallic foams for biodegradable bone replacement materials, Journal of Porous Materials 21 (2014) 131-140.

[133] J. Banhart, M.F. Ashby, N.A. Fleck, Metal foams and porous metal structures, in processing of International Conference on Metal Foams and Porous Metal Structures, Bremen, Germany, 14-16 June, 1999.

[134] D.S. Schwartz, D.S. Shih, A.G. Evans, H.N. Wadley, Porous and cellular materials for structural applications, in processing of Materials Research Society, Symposium Proceedings Volume 521, San Francisco, California, U.S.A, 13-15 April 1998.

[135] K.S.W. Sing, D.H. Everett, R.A.W. Haul, L. Moscou, R.A. Pierotti, J. Rouquerol, T. Siemieniewska, Reporting physisorption data for gas solid systems with special reference to the determination of surface-area and porosity (recommendations 1984), Pure and Applied Chemistry 57 (1985) 603-619.

[136] J. Erlebacher, M.J. Aziz, A. Karma, N. Dimitrov, K. Sieradzki, Evolution of nanoporosity in dealloying, Nature 410 (2001) 450-453.

[137] I. McCue, E. Benn, B. Gaskey, J. Erlebacher, Dealloying and Dealloyed Materials, Annual Review of Materials Research, 46 (2016) 263-286.

[138] A. Katagiri, M. Nakata, Preparation of a high surface area nickel electrode by alloying and dealloying in a $ZnCl_2$-NaCl melt, Journal of the Electrochemical Society 150 (2003) C585-C590.

[139] T. Fukumizu, F. Kotani, A. Yoshida, A. Katagiri, Electrochemical formation of porous nickel in zinc chloride-alkali chloride melts, Journal of the Electrochemical Society 153 (2006) C629-C633.

[140] M. Hakamada, M. Takahashi, T. Furukawa, M. Mabuchi, Coercivity of nanoporous Ni produced by dealloying, Applied Physics Letters 94 (2009) 153105.

[141] K. Brunelli, M. Dabala, R. Frattini, M. Magrini, Structural characterization and electrocatalytic properties of $Au_{30}Zr_{70}$ amorphous alloy obtained by rapid quenching, Journal of Applied Electrochemistry 33 (2003) 995-1000.

[142] Y. Ding, J. Erlebacher, Nanoporous metals with controlled multimodal pore size distribution, Journal of the American Chemical Society 125 (2003) 7772-7773.

[143] Z. Liu, P.C. Searson, Single nanoporous gold nanowire sensors, The Journal of Physical Chemistry B 110 (2006) 4318-4322.

[144] F.L. Jia, C.F. Yu, K.J. Deng, L.Z. Zhang, Nanoporous metal (Cu, Ag, Au) films with high surface area: general fabrication and preliminary electrochemical performance, Journal of Physical Chemistry C 111 (2007) 8424-8431.

[145] F.L. Jia, C.F. Yu, Z.H. Ai, L.Z. Zhang, Fabrication of nanoporous gold film electrodes with ultrahigh surface area and electrochemical activity, Chemistry of Materials 19 (2007) 3648-3653.

[146] J.T. Zhang, P.P. Liu, H.Y. Ma, Y. Ding, Nanostructured porous gold for methanol electro-oxidation, Journal of Physical Chemistry C 111 (2007) 10382-10388.

[147] C.F. Yu, F.L. Jia, Z.H. Ai, L.Z. Zhang, Direct oxidation of methanol on self-supported nanoporous gold film electrodes with high catalytic activity and stability, Chemistry of Materials 19 (2007) 6065-6067.

[148] J. Snyder, K. Livi, J. Erlebacher, Dealloying silver/gold alloys in neutral silver nitrate solution: porosity evolution, surface composition, and surface oxides, Journal of the Electrochemical Society 155 (2008) C464-C473.

[149] L.Y. Chen, J.S. Yu, T. Fujita, M.W. Chen, Nanoporous copper with tunable nanoporosity for SERS applications, Advanced Functional Materials 19 (2009) 1221-1226.

[150] S. Sattayasamitsathit, P. Thavarungkul, C. Thammakhet, W. Limbut, A. Numnuam, C. Buranachai, P. Kanatharana, Fabrication of nanoporous copper film for electrochemical detection of glucose, Electroanalysis 21 (2009) 2371-2377.

[151] X.G. Wang, Z. Qi, C.C. Zhao, W.M. Wang, Z.H. Zhang, Influence of alloy composition and dealloying solution on the formation and microstructure of monolithic nanoporous silver through chemical dealloying of Al-Ag alloys, Journal of Physical Chemistry C 113 (2009) 13139-13150.

[152] A. Jaron, Z. Zurek, New porous iron electrode for hydrogen evolution - production and properties, Archives of Metallurgy and Materials 53 (2008) 847-853.

[153] A. Antoniou, D. Bhattacharrya, J.K. Baldwin, P. Goodwin, M. Nastasi, S.T. Picraux, A. Misra, Controlled nanoporous Pt morphologies by varying deposition parameters, Applied Physics Letters 95 (2009) 073116.

[154] M. Hakamada, H. Nakano, T. Furukawa, M. Takahashi, M. Mabuchi, Hydrogen storage properties of nanoporous palladium fabricated by dealloying, The Journal of Physical Chemistry C 114 (2010) 868-873.

[155] Y. Ding, A. Mathur, M. Chen, J. Erlebacher, Epitaxial casting of nanotubular mesoporous platinum, Angewandte Chemie International Edition 44 (2005) 4002-4006.

[156] M.M. Biener, J. Ye, T.F. Baumann, Y.M. Wang, S.J. Shin, J. Biener, A.V. Hamza, Ultra-strong and low-density nanotubular bulk materials with tunable feature sizes, Advanced Materials 26 (2014) 4808-4813.

[157] Y. Ito, Y. Tanabe, H.J. Qiu, K. Sugawara, S. Heguri, N.H. Tu, K.K. Huynh, T. Fujita, T. Takahashi, K. Tanigaki, High-quality three-dimensional nanoporous graphene, Angewandte Chemie International Edition 53 (2014) 4822-4826.

[158] Y. Ito, Y. Tanabe, J. Han, T. Fujita, K. Tanigaki, M. Chen, Multifunctional porous graphene for high-efficiency steam generation by heat localization, Advanced Materials 27 (2015) 4302-4307.

[159] T. Wada, H. Kato, Three-dimensional open-cell macroporous iron, chromium and ferritic stainless steel, Scripta Materialia 68 (2013) 723-726.

[160] T. Wada, T. Ichitsubo, K. Yubuta, H. Segawa, H. Yoshida, H. Kato, Bulk-nanoporous-silicon negative electrode with extremely high cyclability for lithium-ion batteries prepared using a top-down process, Nano Letters 14 (2014) 4505-4510.

[161] I. McCue, S. Ryan, K. Hemker, X.D. Xu, N. Li, M.W. Chen, J. Erlebacher, Size effects in the mechanical properties of bulk bicontinuous Ta/Cu nanocomposites made by liquid metal dealloying, Advanced Engineering Materials 18 (2016) 46-50.

[162] J.W. Kim, M. Tsuda, T. Wada, K. Yubuta, S.G. Kim, H. Kato, Optimizing niobium dealloying with metallic melt to fabricate porous structure for electrolytic capacitors, Acta Materialia 84 (2015) 497-505.

[163] Y.D. Xie, D.G. Kocaefe, C.Y. Chen, Y. Kocaefe, Review of research on template methods in preparation of nanomaterials, Journal of Nanomaterials 2016 (2016) 11.

[164] T. Niendorf, F. Brenne, P. Hoyer, D. Schwarze, M. Schaper, R. Grothe, M. Wiesener, G. Grundmeier, H.J. Maier, Processing of new materials by additive manufacturing: iron-based alloys containing silver for biomedical applications, Metallurgical and Materials Transactions A 46 (2015) 2829-2833.

[165] A. Bandyopadhyay, B.V. Krishna, W. Xue, S. Bose, Application of laser engineered net shaping (LENS) to manufacture porous and functionally graded structures for load bearing implants, Journal of Materials Science: Materials in Medicine 20 (2009) S29-S34.

[166] O. Näth, A. Stephen, J. Rösler, F. Vollertsen, Structuring of nanoporous nickel-based superalloy membranes via laser etching, Journal of Materials Processing Technology 209 (2009) 4739-4743.